Table 1 List of genes differentially expressed in YB-1 siRNA-transfected SKOV-3 cells

Unigene	*Accession*	*Symbol*	*Description*	*Mean fold change*
Hs.489033	NM_000927	ABCB1	MDR1, ATP-binding cassette, sub-family B (MDR/TAP), member 1	2.46
Hs.369762	AB077208	TYMS	Thymidylate synthetase	1.71
Hs.198363	NM_018518	MCM10	MCM10 minichromosome maintenance deficient 10	1.70
Hs.405958	U77949	CDC6	CDC6 cell division cycle 6 homolog (*S. cerevisiae*)	1.66
Hs.442658	AB011446	AURKB	Aurora kinase B	1.65
Hs.516484	NM_005978	S100A2	S100 calcium-binding protein A2	1.48
Hs.23960	NM_031966	CCNB1	Cyclin B1	1.40
Hs.460184	AA604621	MCM4	MCM4 minichromosome maintenance deficient 4 (*S. cerevisiae*)	1.40
Hs.438720	AF279900	MCM7	MCM7 minichromosome maintenance deficient 7 (*S. cerevisiae*)	1.36
Hs.433168	NM_002960	S100A3	S100 calcium binding protein A3	1.33
Hs.115474	NM_002915	RFC3	Replication factor C (activator 1) 3, 38 kDa	1.28
Hs.122908	NM_030928	CDT1	DNA replication factor	1.28
Hs.329989	NM_005030	PLK1	Polo-like kinase 1 (*Drosophila*)	1.21
Hs.334562	NM_001786	CDC2	Cell division cycle 2, G1 to S and G2 to M	1.21
Hs.74034	NM_001753	CAV1	Caveolin 1, caveolae protein, 22 kDa	1.19
Hs.477481	NM_004526	MCM2	MCM2 minichromosome maintenance deficient 2, mitotin	1.16
Hs.284244	M27968	FGF2	Fibroblast growth factor 2 (basic)	1.10
Hs.179565	NM_002388	MCM3	MCM3 minichromosome maintenance deficient 3 (*S. cerevisiae*)	1.08
Hs.194698	NM_004701	CCNB2	Cyclin B2	1.04
Hs.506989	BC001866	RFC5	Replication factor C (activator 1) 5, 36.5 kDa	1.02
Hs.171596	NM_004431	EPHA2	EPH receptor A2	1.01
Hs.194143	NM_007294	BRCA1	Breast cancer 1, early onset	0.75
Hs.156346	NM_001067	TOP2A	Topoisomerase (DNA) II alpha 170 kDa	0.64
Hs.473163	NM_001719	BMP7	Bone morphogenetic protein 7 (osteogenic protein 1)	0.54
Hs.391464	NM_004996	ABCC1	MRP-1, ATP-binding cassette, sub-family C (CFTR/MRP), member 1	0.20
Hs.256301	NM_199249	MGC13170	Multidrug resistance-related protein	0.15
Hs.513488	NM_017458	MVP	Major vault protein	−0.05
Hs.482526	NM_014886	TINP1	TGF beta-inducible nuclear protein 1	−0.23
Hs.525557	NM_000295	SERPINA1	Serpin peptidase inhibitor, clade A (alpha-1 antiproteinase, antitrypsin), member	−1.01
Hs.500466	BG403361	PTEN	Phosphatase and tensin homolog (mutated in multiple advanced cancers 1)	−1.05
Hs.25292	NM_002229	JUNB	Jun B proto-oncogene	−1.06
Hs.132225	AI934473	PIK3R1	Phosphoinositide-3-kinase, regulatory subunit, polypeptide 1 (p85 alpha)	−1.16
Hs.83169	NM_002421	MMP1	Matrix metalloproteinase 1 (interstitial collagenase)	−1.22
Hs.508999	NM_002742	PRKCM	Protein kinase C, mu	−1.29
Hs.326035	NM_001964	EGR1	Early growth response 1	−1.29
Hs.2256	NM_002423	MMP7	Matrix metalloproteinase 7 (matrilysin, uterine)	−1.32
Hs.197922	NM_018584	CaMKIINalpha	Calcium/calmodulin-dependent protein kinase II	−1.36
Hs.132966	AA005141	MET	Met proto-oncogene (hepatocyte growth factor receptor)	−1.39
Hs.208124	NM_000125	ESR1	Estrogen receptor 1	−1.50
Hs.73793	M27281	VEGF	Vascular endothelial growth factor	−1.53
Hs.381167	AW512196	SERPINB1	Serine (or cysteine) proteinase inhibitor, clade B (ovalbumin), member 1	−1.70
Hs.413111	NM_002661	PLCG2	Phospholipase C, gamma 2 (phosphatidylinositol-specific)	−1.75
Hs.461086	NM_004360	CDH1	Cadherin 1, type 1, E-cadherin (epithelial)	−1.92
Hs.472793	AI631895	SGK2	Serum/glucocorticoid regulated kinase 2	−2.04
Hs.372914	NM_006096	NDRG1	*N-myc* downstream regulated gene 1	−2.34
Hs.421986	NM_001008540	CXCR4	Chemokine (C-X-C motif) receptor 4	−2.64

High-density oligonucleotide array was performed on 400 nM YB-1 siRNA-treated SKOV-3 cells and mock-treated cells. siRNA duplexes were transfected using LipofectAMINE2000 with Opti-MEM mediums. At 48 h after siRNA transfection, total RNA was prepared, and subjected to double-stranded cDNA synthesis and *in vitro* transcription. The labeled cRNA was applied to the oligonucleotide microarray.

respectively, and silencing effects of siRNA were analysed by immunoblotting (Figure 6a). In Akt siRNA almost completely silenced both Akt1 and Akt2, and siRNA for ILK, the upstream kinase for Akt, silenced ILK on protein level. Treatment with Akt siRNA and ILK siRNA resulted in a marked decrease in both pAkt expression and nuclear accumulation of YB-1 (Figure 6a). As both Akt and ILK siRNA blocked the nuclear translocation of YB-1, we examined their effects on expression of YB-1-regulated genes (Figure 6b). Treatment with Akt and ILK siRNA downregulated the expression of *CXCR4* gene, and upregulated the expression of *MDR1* gene. By contrast there appeared no marked effect on the expression of *MVP/LRP* and *YB-1* genes when treated with both siRNAs (Figure 6b).

Effect of LY294002 treatment on Akt phosphorylation and YB-1 nuclear localization in SKOV-3 xenograft

To further investigate the involvement of Akt in tumoural YB-1 nuclear localization, an *in vivo* xenograft

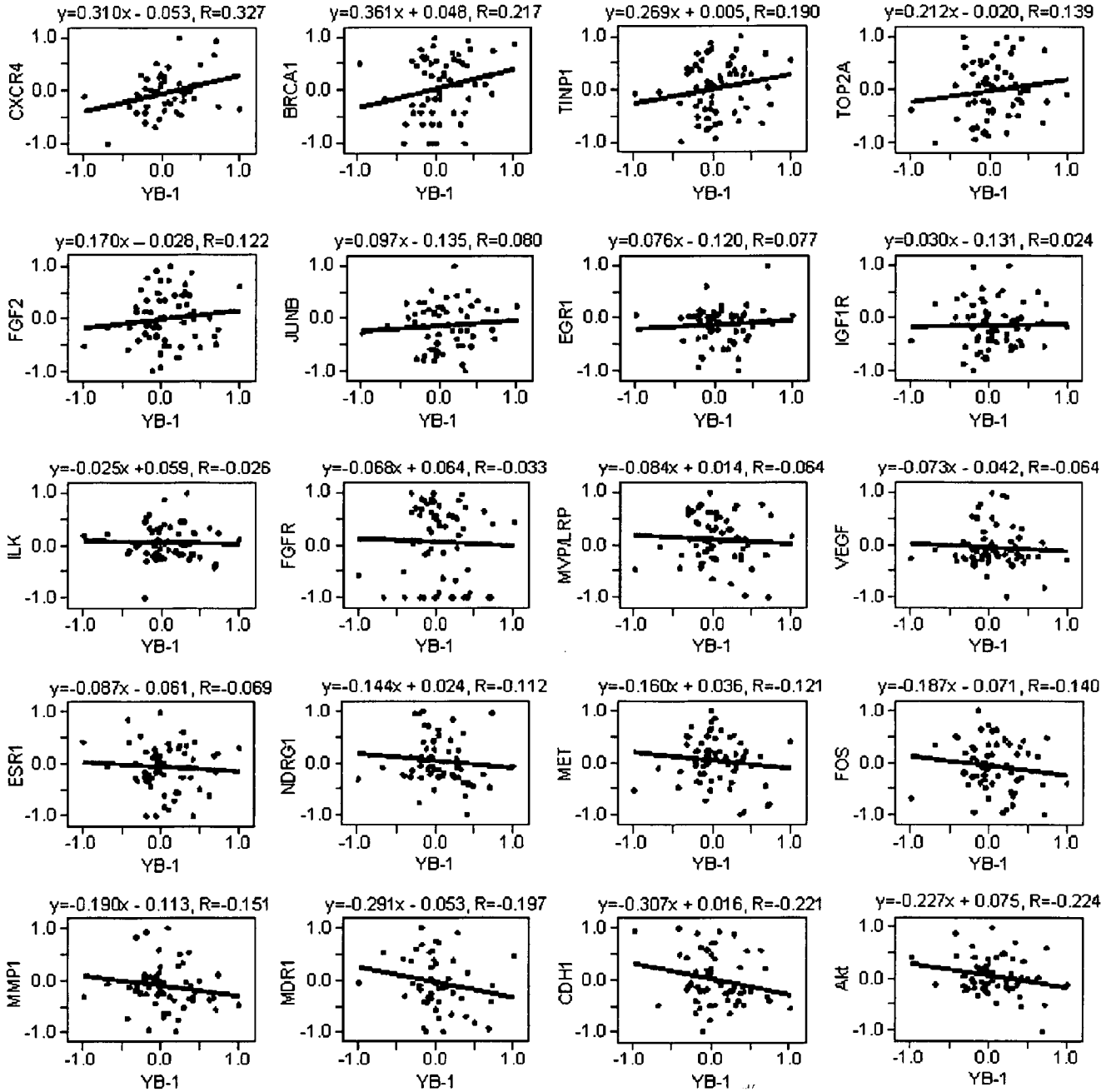

Figure 3 Correlation analysis of gene expression in NCI-60 screen. Gene expression data for the 60 human tumor cell lines were obtained from the Developmental Therapeutics Program (http://www.dtp.nci.nih.gov/), expressed as log of the mRNA levels in cell line/mRNA levels in reference pool in the NCI screen. Pearson correlation coefficients were calculated for each gene–gene pair.

assay was performed. Administration of LY294002 (i.p.) to mice carrying SKOV-3 cell tumors inhibited the phosphorylation of Akt (Figure 7a and b). Akt phosphorylation and YB-1 nuclear localization were also evaluated by immunohistochemical analysis. Tumors in the LY294002-treated group displayed a lower level of pAkt staining (3.3 ± 0.5) than those in the control group, where the mean number of nuclear YB-1-positive cells was 24.7 ± 3.4 (Figure 7c and d). Taken together, these results suggest that nuclear localization of YB-1 in ovarian cancer cells is closely associated with Akt phosphorylation activity *in vitro* and *in vivo*.

Discussion

The nuclear localization of YB-1 is essential process for YB-1-driven transcription of various genes and DNA repair in cancer cells in response to various environmental stimuli. One should understand which signalling pathway specifically controls the translocation of YB-1 from cytoplasm into nucleus. Our previous study has demonstrated that PKC activates the nuclear localization of YB-1 in cancer cells treated with UV irradiation or cisplatin, and also that the C-terminal region of YB-1 was important for its cytoplasmic

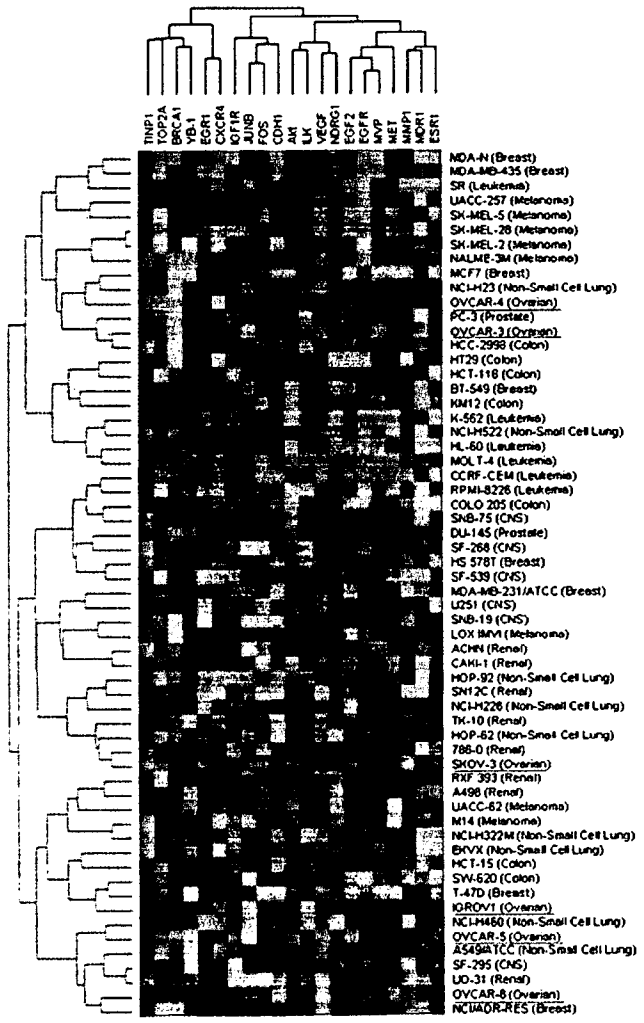

Figure 4 Hierarchical clustering of gene expression in NCI-60 screen. Hierarchical clustering can be used to group cell lines and genes in term of their patterns of gene expression. To obtain cluster trees for genes that showed distinct expression patterns across the 60 cell lines, we used the program 'Cluster' and 'Tree View' (http://rana.lbl.gov/) with average linkage clustering and a correlation metric.

retention (Koike *et al.*, 1997). Sutherland *et al.* (2005) have presented more definitive mechanism at molecular basis that phosphorylation of serine 102 at cold-shock domain of YB-1 by Akt is essential for the nuclear YB-1 localization in breast cancer cells, and also that ILK phosphorylate its downstream Akt, resulting in activation of YB-1 and it nuclear localization. Consistent with this study, our present study also demonstrated that Akt as well as ILK played a critical role in the nuclear YB-1 localization and YB-1-driven-transcriptional control of various genes including *CXCR4* and *MDR1* in human ovarian cancer cells.

In our present study, we examined whether expression of two multidrug resistance relevant genes, *MVP/LRP* and *MDR1/ABCB1*, was affected by knockdown of YB-1. Stein *et al.* (2005) have reported that the *MVP/LRP* gene is transcriptionally activated by YB-1 in response to cytotoxic anticancer agents including doxorubicin and 5-fluorouracil: *MVP/LRP* is an essential vault protein involving acquirement of multidrug resistance. However, in ovarian cancer cells, there was no causative association between the two genes when assayed by microarray and QRT-PCR. YB-1 might not regulate *MVP/LRP* expression in ovarian cancer cells used in our present study. In contrast, in human breast cancer cells, treatment with YB-1 siRNA markedly upregulated *MVP/LRP* expression (Shimoyama T, Nishio K, Basaki Y, Ono M and Kuwano M, unpublished data), suggesting that YB-1-induced regulation of *MVP/LRP* gene expression depends upon cancer cell types and/or types of stimuli. In contrast, knockdown or nuclear translocation inhibition of YB-1 upregulated expression of another drug resistance *MDR1* gene in ovarian cancer cells. Various environmental stimuli often upregulated *MDR1* gene in various human cancer cells through pleiotropic transcriptional regulations (Kuwano *et al.*, 2004). Our present study further presented a novel regulation of YB-1-induced negative control of *MDR1* gene in ovarian cancer cells, and further study should be required to understand its underlying mechanism at molecular basis.

In our present study, we first observed that the knockdown of YB-1, ILK and Akt as well as an Akt inhibitor all downregulated expression of *CXCR4* gene. Consistent with recent study by Sutherland *et al.* (2005), ILK-Akt activation could be responsible for the nuclear localization of YB-1, resulting in enhanced expression of *CXCR4* gene. The 2.6 Kb 5′-flanking region located upstream of the *CXCR4* gene contains a TATA box and the transcription start site characteristic of a functional promoter (Caruz *et al.*, 1998) and this region also contained putative consensus Y-box-binding site (inverted CCAAT box) form −685 to −681. However, it remains unknown whether ILK-Akt-induced activation of YB-1 is directly involved in the upregulation of *CXCR4* gene.

CXCL12 (SDF-1α) is a specific ligand of CXCR4. CXCL12 induced a dose dependent proliferation of human ovarian cancer cells through its specific interaction with CXCR4 (Porcile *et al.*, 2005). This CXCR4 activation by CXCL12 further stimulated EGF receptor phosphorylation and its downstream kinases, ERK1/2, Akt and c-Src that might link several signallings of cell proliferation in ovarian cancer cells (Porcile *et al.*, 2005). On the other hand, VEGF, a potent angiogenic factor, induced upregulation of *CXCR4* gene expression in vascular endothelial cells, and expression of both VEGF and CXCL12 was very high in ascites of patients with advanced ovarian cancers (Kryczek *et al.*, 2005). The cross-talk of CXCL12/CXCR4 with EGF/EGF receptor and/or VEGF/VEGF receptor might thus provide important signallings for both cell proliferation and angiogenesis in ovarian cancers.

CXCL12/CXCR4 pathway is also expected to be clinically involved in acquirement of malignant characteristics of human ovarian cancers. Of 14 chemokine receptors, only CXCR4 protein was found to be expressed in ovarian cancer cell lines and in ascites from patients with ovarian cancers (Scotton *et al.*, 2001). The CXCL12/CXCR4 pathway has been implicated in

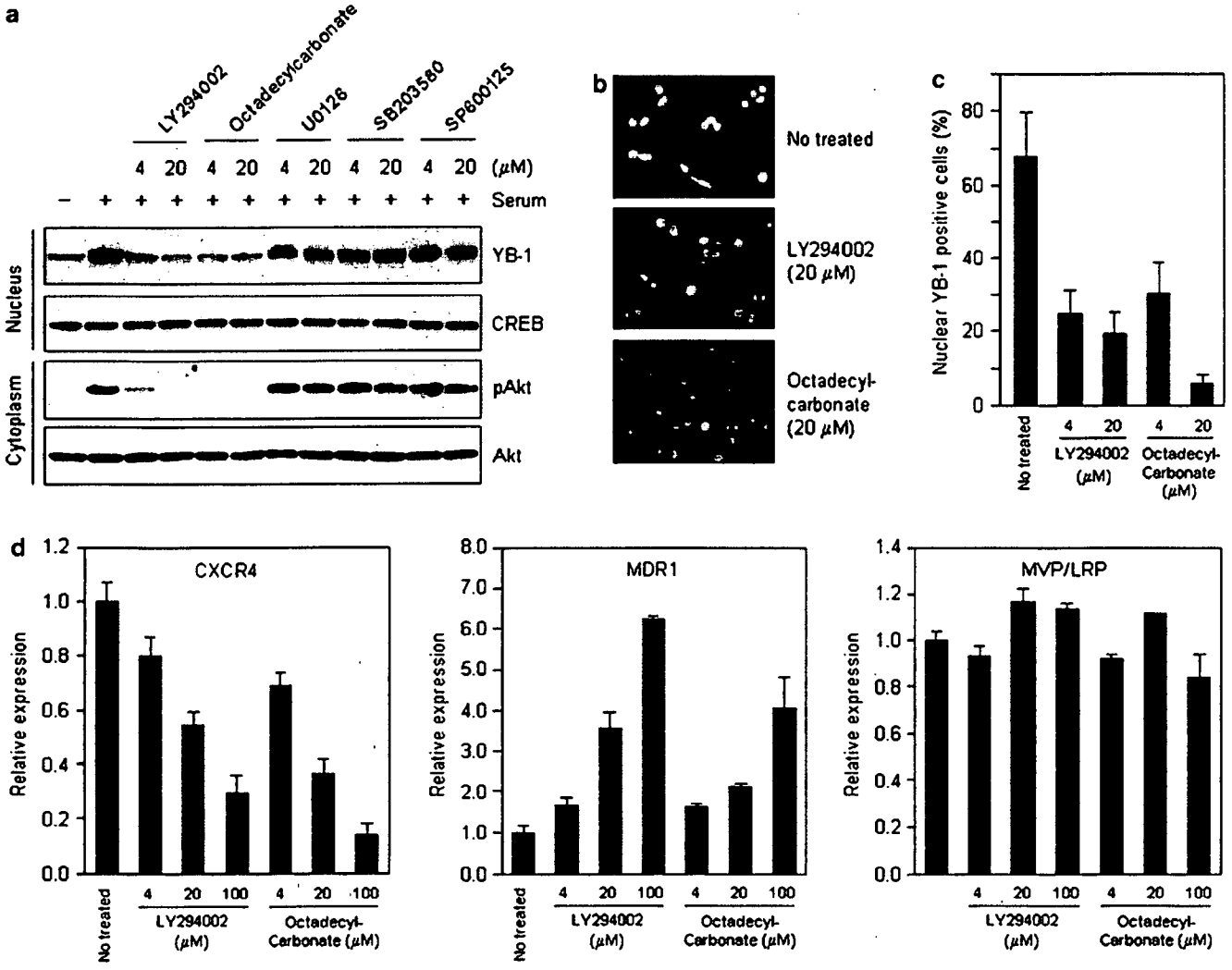

Figure 5 Akt activity is required for YB-1 nuclear accumulation and transcriptional regulation by YB-1. (**a**) The effect of kinase inhibitors on the nuclear accumulation of YB-1 in SKOV-3 cells. Inhibitors were added 3 h before serum stimulation and nuclear extracts were prepared 1 h after serum stimulation. Anti-YB-1 and anti-CREB immunoblots were performed with nuclear extracts, and anti-pAkt and anti-Akt immunoblots were performed on cytoplasmic extracts. CREB and Akt are shown as a loading control. (**b**) Immunofluorescent staining for YB-1. SKOV-3 cells were treated with LY294002 or octadecylcarbonate for 24 h and then stained with YB-1. Cells were fixed and permeabilized, incubated at 4°C with the primary YB-1 antibody, then with the Alexa Flour 546-labelled secondary antibody. (**c**) Quantitative analysis of YB-1 nuclear localization in SKOV-3 cells as shown in Figure 2b. Data are mean of three independent experiments; bars ±s.d. (**d**) QRT-PCR for MDR1, MVP/LRP, CXCR4 and housekeeping gene GAPDH. The relative gene expression for each sample was determined using the formula $2^{(-\Delta C_t)} = 2^{(C_t(\text{GAPDH}) - C_t(\text{target}))}$ which reflected target gene expression normalized to GAPDH levels. Data were mean of three independent experiments; bars ±s.d.

the development of tumor growth, angiogenesis and metastasis not only in ovarian cancer (Scotton *et al.*, 2002) but also in other tumor types including breast cancer (Muller *et al.*, 2001), melanoma (Robledo *et al.*, 2001; Murakami *et al.*, 2002) and prostate cancer (Darash-Yahana *et al.*, 2004). Jiang *et al.* (2006) further demonstrated that CXCR4 expression could be an important prognostic marker for ovarian cancers: the rate of CXCR4 expression in refractory and recurrent group was significantly higher than that in non-recurrent group. Our previous studies showed a significant association of nuclear localization of YB-1 with unfavorable prognosis of patients with ovarian cancers (Kamura *et al.*, 1999; Huang *et al.*, 2004). Clinicopathological analysis whether nuclear expression of YB-1 can be associated with CXCR4 expression or CXCL12 (SDF-1α) in patients with ovarian cancers is now in progress.

Several studies have focused on the role of Akt/PI3K inhibitors as potential tumor suppressor agents. It has been reported that phosphorylation of Akt and mTOR, an Akt substrate, was frequently detected in ovarian cancer (Altomare *et al.*, 2004). In animal model of ovarian cancer, LY294002, a potent inhibitor of Akt activation, could inhibit cancer growth and ascites formation (Hu *et al.*, 2000). Our study also

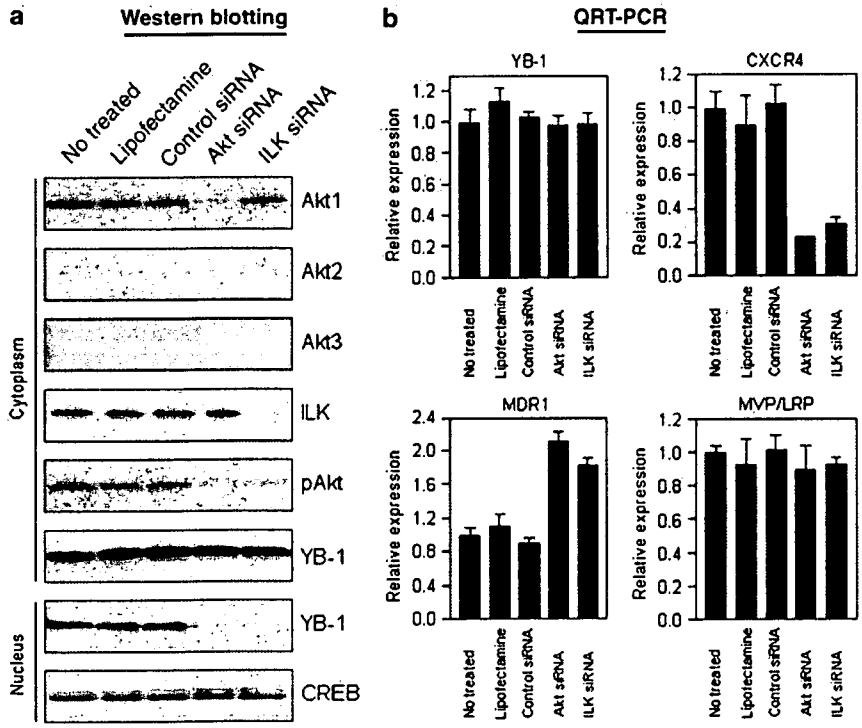

Figure 6 Effect of knock down of Akt and ILK on YB-1 nuclear accumulation, and expression of MDR1, MVP/LRP and CXCR4. (**a**) SKOV-3 cells were treated with Akt siRNA (100 nM), ILK siRNA (10 nM) or control siRNA (100 nM) for 48 h, and then cytoplasmic and nuclear extracts were prepared. Anti-Akt1, anti-Akt2, anti-Akt3, anti-ILK, anti-pAkt, and anti-YB-1 immunoblots were performed with cytoplasmic extracts, and anti-YB-1 and anti-CREB immunoblots were performed with nuclear extracts. (**b**) SKOV-3 cells were treated with Akt siRNA (100 nM) or ILK siRNA (10 nM) for 48 h and then total RNA was prepared. QRT-PCR was performed for MDR1, MVP/LRP, CXCR4, YB-1 and GAPDH housekeeping gene. The relative gene expression for each sample was determined using the formula $2^{(-\Delta C_t)} = 2^{(C_t(\text{GAPDH}) - C_t(\text{target}))}$ which reflected target genes normalized to GAPDH levels. Data were mean of three independent experiments; bars ±s.d.

demonstrated that both Akt phosphorylation and YB-1 nuclear localization were blocked by administration of LY294002 in SKOV-3 xenograft model. Nuclear localization of YB-1 is induced through various pathways including Akt (see Introduction). The Akt-dependent pathway for YB-1 nuclear localization would provide further insight how Akt-targeting anticancer therapeutic strategy could be developed.

In conclusion, we have identified several genes that are regulated by YB-1 and/or its nuclear localization. Further immunohistochemical analysis should be required to elucidate the role of YB-1 in the expression of *CXCR4* and other relevant genes that are associated with the clinicopathological characteristics in human ovarian cancers. Based on our present experimental results, we aim to present YB-1 and YB-1-dependent gene networks as molecular targets for the further development of novel anticancer therapeutic strategies.

Materials and methods

Cell culture and reagents

OVCAR-3 and SKOV-3 were purchased from American Type Culture Collection (Manassas, VA, USA). RMG-I, RMG-II, RMG-III, RMBG and RTSG were kindly provided by Dr S Nozawa, Department of Obstetrics and Gynecology, Keio University. These cell lines were grown in DMEM supplemented with 10% fetal bovine serum (FBS) in an atmosphere of 5% CO_2. LY294002 and U0126 were purchased from Sigma Chemical Co. (St Louis, MO, USA). 1L-6-hydroxymethyl-*chiro*-inositol 2(*R*)-2-*O*-methyl-3-*O*-octadecylcarbonate (Hu *et al*., 2000), SB203580 (Cuenda *et al*., 1995), and SP600125 (Bennett *et al*., 2001) were obtained from Calbiochem (San Diego, CA, USA). Anti-YB-1 was generated as described previously (Ohga *et al*., 1996). Anti-CREB, anti-PKB/Akt, anti-phospho-PKB/Akt, anti-ILK, Akt siRNA and ILK siRNA were obtained from Cell Signaling Technology (Beverly, MA, USA).

Western blotting

Western blotting was performed as previously described (Kaneko *et al*., 2004). Cells were lysed in buffer A (10 mM HEPES (pH7.9), 10 mM KCl, 10 mM EDTA, 1 mM DTT, 0.4% v/v IGEPAL, 1 mM Na_3VO_4, 1 mM PMSF, and 10 μg/ml aprotinin and leupeptin) for 10 min on ice, and then centrifuged for 3 min at 15 000 r.p.m. The supernatant fractions (cytoplasmic soluble proteins) were collected. The nuclear pellet was then washed and then lysed in buffer C (20 mM HEPES (pH7.9), 200 mM NaCl, 1 mM EDTA, 5% v/v glycerol, 1 mM DTT, 1 mM Na_3VO_4, 1 mM PMSF and 10 μg/ml aprotinin and leupeptin). Lysates were incubated on ice for 2 h, and then centrifuged 15 000 r.p.m. for 5 min. The lysates were separated by sodium dodecyl sulfate–polyacryl amide gel electrophoresis (SDS–PAGE), and then were transferred to a nitrocellulose membrane. The membrane were incubated with the primary antibody and visualized with secondary antibody coupled to horseradish peroxidase (Cell Signaling Technology)

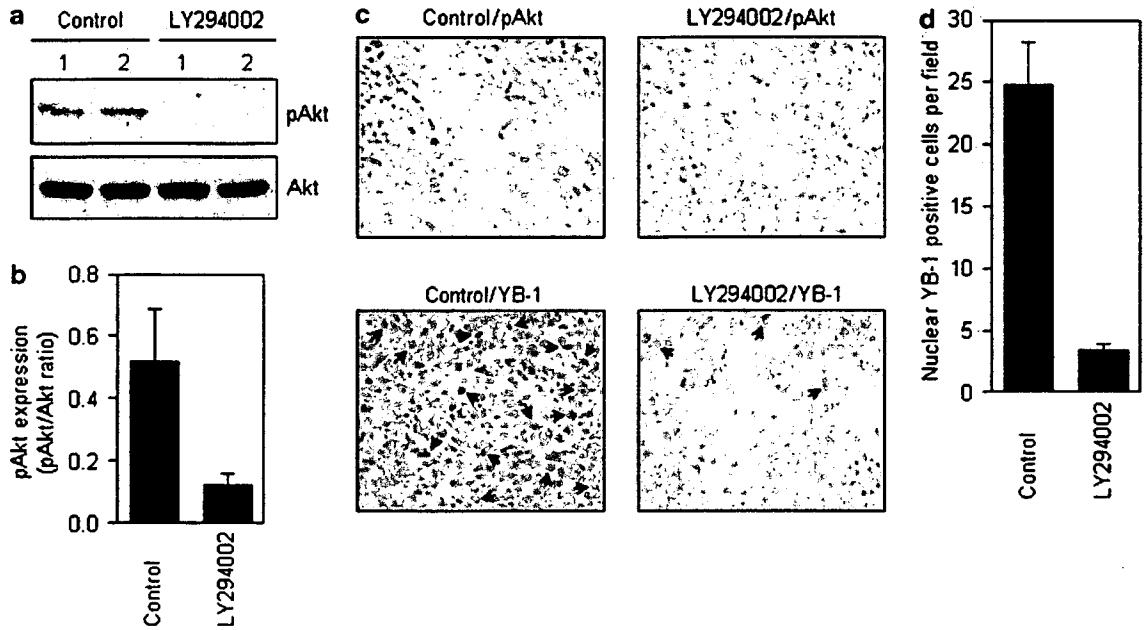

Figure 7 Effect of LY294002 on Akt phosphorylation and YB-1 nuclear localization in SKOV-3 xenograft. (**a**) Effect of LY294002 on Akt phosphorylation in SKOV-3 xenograft. SKOV-3 cells were injected subcutaneously (5.0×10^6 cells/0.1 ml/mouse). When tumors reached approximately 1000–2000 mm^3, animals were randomly assigned to two groups of five. The first group received i.p. injections of DMSO as a control. The second group received i.p. injections of 50 mg/kg LY294002. One hour after LY294002 injection, mice were killed humanely (while anesthetized) by cervical dislocation and tumors were excised. Western blot analysis was carried out using cytosolic extracts prepared from tumor tissues from two animals treated with or without drug. (**b**) Quantitative analysis of Akt phosphorylation in SKOV-3 tumor xenograft. Levels of Akt phosphorylation were normalized to their nonphosphorylated form as shown in Figure 7a. Data are expressed as mean ± s.d. of three to five mice. (**c**) Immunohistochemical staining was carried out using conventional protocols. The arrows indicate positive cell nuclei staining for YB-1 (× 200 magnification). (**d**) Quantitative analysis of YB-1 nuclear localization in SKOV-3 tumor xenograft. YB-1 nuclear localization was determined by counting the number of positive YB-1 nuclear cells in high-power fields as shown in Figure 7b. Data were mean of each section (five sections per mouse). Columns, mean; bars ± s.d.

and SuperSignal West Pico Chemiluminescent Substrate (Pierce, Rockford, IL, USA). Bands on Western blots were analysed densitometrically using Scion Image software (version 4.0.2; Scion Corp., Frederick, MD, USA).

Oligonucleotide microarray analysis

The siRNA corresponding to nucleotide sequences of the YB-1 (5′-GGU UCC CAC CUU ACU ACA U-3′) was purchased from QIAGEN Inc. (Valencia, CA, USA). A negative control siRNA was obtained from Invitrogen (Carlsbad, CA, USA). siRNA duplexes were transfected using LipofectAMINE2000 and Opti-MEM medium (Invitrogen) according to the manufacturer's recommendations. Duplicate samples were prepared for microarray hybridization. At 48 h after siRNA transfection, total RNA was extracted from cell cultures using ISOGEN (Nippon Gene Co. Ltd., Tokyo, Japan). Total RNA (2 μg) was reverse-transcribed using GeneChip 3′-Amplification Reagents One-Cycle cDNA Synthesis Kit (Affymetrix Inc., Santa Clara, CA, USA) and then labeled with Cy5 or Cy3. The labeled cRNA was applied to the oligonucleotide microarray (Human Genome U133 Plus 2.0 Array, Affymetrix). The microarray was scanned on a GeneChip Scanner3000 and the image was analysed using a GeneChip Operating Software ver1.

Correlation analysis of gene expression, and clustering of cell lines and genes expression

Gene expression data for the 60 human tumor cell lines were obtained from the Developmental Therapeutics Program (http://www.dtp. nci.nih.gov/), expressed as log of the mRNA levels in cell line/mRNA levels in reference pool in the NCI screen. Pearson correlation coefficients were calculated for each gene–gene pair. Hierarchical clustering can be used to group cell lines and genes in term of their patterns of gene expression. To obtain cluster trees for genes that showed distinct expression patterns across the 60 cell lines, we used the program 'Cluster' and 'Tree View' (http://rana.lbl.gov/) with average linkage clustering and a correlation metric (Eisen *et al.*, 1998).

Quantitative real-time polymerase chain reaction

RNA was reverse transcribed from random hexamers using AMV reverse transcriptase (Promega, Madison, WI, USA). Real-time quantitative PCR was performed using the Real-Time PCR system 7300 (Applied Biosystems, Foster City, CA, USA) as described previously (Maruyama *et al.*, 2006). In brief, the PCR amplification reaction mixtures (20 μl) contained cDNA, primer pairs, the dual-labeled fluorogenic probe, and TaqMan Universal PCR Master Mix (Applied Biosystems). The thermal cycle conditions included maintaining the reactions at 50°C for 2 min and at 95°C for 10 min, and then alternating for 40 cycles between 95°C for 15 s and 60°C for 1 min. The primer pairs and the probe were obtained from Applied Biosystems. The relative gene expression for each sample was determined using the formula $2^{(-\Delta C_t)} = 2^{(C_t(\mathrm{GAPDH}) - C_t(\mathrm{target}))}$ which reflected target gene expression normalized to GAPDH levels.

Immunofluorescence

Cells were plated on glass coverslips in six-well plates and allowed to attach overnight. Then, cells were rinsed with PBS

and then fixed in 4% paraformaldehyde/PBS for 30 min. Cells were rinsed twice with PBS and then permeabilized with 0.5 ml of solution containing 5% BSA, 0.2% Triton X-100 in PBS for 90 min. After 1 h of blocking with 2% goat serum, the cells were incubated overnight with primary antibody at 4°C in 1% BSA in PBS. Cells were then rinsed three times with PBS and incubated with 1 μg/ml of Alexa Flour 546-labeled secondary antibody (Molecular Probe, Eugene, OR, USA) in 1% BSA in PBS for 60 min. Coverslips were mounted on slide glasses using gel mount and viewed using an Olympus BX51 florescence microscope (Tokyo, Japan) and photographed with Olympus DP-70 digital camera.

Tumor xenograft study

Male BALB/c nude mice were obtained from Kyudo Co., Ltd. (Fukuoka, Japan). SKOV-3 cells were harvested and resuspended in PBS. The suspension was injected subcutaneously in the mice (5.0×10^6 cells/0.1 ml/mouse). When tumors reached about 1000–2000 mm^3, animals were randomly assigned to two groups of five mice each. The first group received i.p. injections of DMSO as control. The second group received i.p. injection of LY294002 at 50 mg/kg. At 1 h after LY294002 injection, mice were killed humanly (mice still anesthetized) by cervical dislocation and tumors were excised. For immunohistchemistry, one part of the tumor tissue was fixed in formalin and embed in paraffin.

Acknowledgements

We thank Y Yamada and Y Yamasaki in Hanno Research Center of Taiho Pharmaceutical Co. Ltd. for fruitful discussion, and N Shinbaru in Kyushu University for editorial help. This study was supported by the COE program for Medical Sciences, Kurume University, and grant-in-aid for scientific research on priority areas cancer from Ministry of Education Culture, Sports Science, and Technology of Japan and the 2nd-Comprehensive Ten-Year Strategy for Cancer Control from the Ministry of Health, Welfare and Labor, Japan.

References

Altomare DA, Wang HQ, Skele KL, De Rienzo A, Klein-Szanto AJ, Godwin AK *et al.* (2004). AKT and mTOR phosphorylation is frequently detected in ovarian cancer and can be targeted to disrupt ovarian tumor cell growth. *Oncogene* **23**: 5853–5857.

Asakuno K, Kohno K, Uchiumi T, Kubo T, Sato S, Isono M *et al.* (1994). Involvement of a DNA binding protein, MDR-NF1/YB-1, in human MDR1 gene expression by actinomycin D. *Biochem Biophys Res Commun* **199**: 1428–1435.

Ashizuka M, Fukuda T, Nakamura T, Shirasuna K, Iwai K, Izumi H *et al.* (2002). Novel translational control through an iron-responsive element by interaction of multifunctional protein YB-1 and IRP2. *Mol Cell Biol* **22**: 6375–6383.

Bargou RC, Jurchott K, Wagener C, Bergmann S, Metzner S, Bommert K *et al.* (1997). Nuclear localization and increased levels of transcription factor YB-1 in primary human breast cancers are associated with intrinsic MDR1 gene expression. *Nat Med* **3**: 447–450.

Bennett BL, Sasaki DT, Murray BW, O'Leary EC, Sakata ST, Xu W *et al.* (2001). SP600125, an anthrapyrazolone inhibitor of Jun N-terminal kinase. *Proc Natl Acad Sci USA* **98**: 13681–13686.

Caruz A, Samsom M, Alonso JM, Alcami J, Baleux F, Virelizier JL *et al.* (1998). Genomic organization and promoter characterization of human CXCR4 gene. *FEBS Lett* **426**: 271–278.

Cuenda A, Rouse J, Doza YN, Meier R, Cohen P, Gallagher TF *et al.* (1995). SB 203580 is a specific inhibitor of a MAP kinase homologue which is stimulated by cellular stresses and interleukin-1. *FEBS Lett* **364**: 229–233.

Darash-Yahana M, Pikarsky E, Abramovitch R, Zeira E, Pal B, Karplus R *et al.* (2004). Role of high expression levels of CXCR4 in tumor growth, vascularization, and metastasis. *FASEB J* **18**: 1240–1242.

Dooley S, Said HM, Gressner AM, Floege J, En-Nia A, Mertens PR. (2006). Y-box protein-1 is the crucial mediator of antifibrotic interferon-gamma effects. *J Biol Chem* **281**: 1784–1795.

Eisen MB, Spellman PT, Brown PO, Botstein D. (1998). Cluster analysis and display of genome-wide expression patterns. *Proc Natl Acad Sci USA* **95**: 14863–14868.

En-Nia A, Yilmaz E, Klinge U, Lovett DH, Stefanidis I, Mertens PR. (2005). Transcription factor YB-1 mediates DNA polymerase alpha gene expression. *J Biol Chem* **280**: 702–711.

Evdokimova V, Ruzanov P, Imataka H, Raught B, Svitkin Y, Ovchinnikov LP *et al.* (2001). The major mRNA-associated protein YB-1 is a potent 5′ cap-dependent mRNA stabilizer. *EMBO J* **20**: 5491–5502.

Fukuda T, Ashizuka M, Nakamura T, Shibahara K, Maeda K, Izumi H *et al.* (2004). Characterization of the 5′-untranslated region of YB-1 mRNA and autoregulation of translation by YB-1 protein. *Nucleic Acids Res* **32**: 611–622.

Furukawa M, Uchiumi T, Nomoto M, Takano H, Morimoto RI, Naito S *et al.* (1998). The role of an inverted CCAAT element in transcriptional activation of the human DNA topoisomerase IIalpha gene by heat shock. *J Biol Chem* **273**: 10550–10555.

Holm PS, Bergmann S, Jurchott K, Lage H, Brand K, Ladhoff A *et al.* (2002). YB-1 relocates to the nucleus in adenovirus-infected cells and facilitates viral replication by inducing E2 gene expression through the E2 late promoter. *J Biol Chem* **277**: 10427–10434.

Hu L, Zaloudek C, Mills GB, Gray J, Jaffe RB. (2000). *In vivo* and *in vitro* ovarian carcinoma growth inhibition by a phosphatidylinositol 3-kinase inhibitor (LY294002). *Clin Cancer Res* **6**: 880–886.

Huang X, Ushijima K, Komai K, Takemoto Y, Motoshima S, Kamura T *et al.* (2004). Co-expression of Y box-binding protein-1 and P-glycoprotein as a prognostic marker for survival in epithelial ovarian cancer. *Gynecol Oncol* **93**: 287–291.

Ise T, Nagatani G, Imamura T, Kato K, Takano H, Nomoto M *et al.* (1999). Transcription factor Y-box binding protein 1 binds preferentially to cisplatin-modified DNA and interacts with proliferating cell nuclear antigen. *Cancer Res* **59**: 342–346.

Jiang YP, Wu XH, Shi B, Wu WX, Yin GR. (2006). Expression of chemokine CXCL12 and its receptor CXCR4 in human epithelial ovarian cancer: an independent prognostic factor for tumor progression. *Gynecol Oncol* **103**: 226–233.

Kamura T, Yahata H, Amada S, Ogawa S, Sonoda T, Kobayashi H *et al.* (1999). Is nuclear expression of Y box-binding protein-1 a new prognostic factor in ovarian serous adenocarcinoma? *Cancer* **85**: 2450–2454.

Kaneko Y, Kitazato K, Basaki Y. (2004). Integrin-linked kinase regulates vascular morphogenesis induced by vascular endothelial growth factor. *J Cell Sci* **117**: 407–415.

Kohno K, Izumi H, Uchiumi T, Ashizuka M, Kuwano M. (2003). The pleiotropic functions of the Y-box-binding protein, YB-1. *Bioessays* **25**: 691–698.

Koike K, Uchiumi T, Ohga T, Toh S, Wada M, Kohno K *et al.* (1997). Nuclear translocation of the Y-box binding protein by ultraviolet irradiation. *FEBS Lett* **417**: 390–394.

Kryczek I, Lange A, Mottram P, Alvarez X, Cheng P, Hogan M *et al.* (2005). CXCL12 and vascular endothelial growth factor synergistically induce neoangiogenesis in human ovarian cancers. *Cancer Res* **65**: 465–472.

Kuwano M, Oda Y, Izumi H, Yang SJ, Uchiumi T, Iwamoto Y *et al.* (2004). The role of nuclear Y-box binding protein 1 as a global marker in drug resistance. *Mol Cancer Ther* **3**: 1485–1492.

Ladomery M, Sommerville J. (1995). A role for Y-box proteins in cell proliferation. *Bioessays* **17**: 9–11.

Maruyama Y, Ono M, Kawahara A, Yokoyama T, Basaki Y, Kage M *et al.* (2006). Tumor growth suppression in pancreatic cancer by a putative metastasis suppressor gene Cap43/NDRG1/Drg-1 through modulation of angiogenesis. *Cancer Res* **66**: 6233–6242.

Matsumoto K, Wolffe AP. (1998). Gene regulation by Y-box proteins: coupling control of transcription and translation. *Trends Cell Biol* **8**: 318–323.

Mossink MH, van Zon A, Scheper RJ, Sonneveld P, Wiemer EA. (2003). Vaults: a ribonucleoprotein particle involved in drug resistance? *Oncogene* **22**: 7458–7467.

Muller A, Homey B, Soto H, Ge N, Catron D, Buchanan ME *et al.* (2001). Involvement of chemokine receptors in breast cancer metastasis. *Nature* **410**: 50–56.

Murakami T, Maki W, Cardones AR, Fang H, Tun Kyi A, Nestle FO *et al.* (2002). Expression of CXC chemokine receptor-4 enhances the pulmonary metastatic potential of murine B16 melanoma cells. *Cancer Res* **62**: 7328–7334.

Ohga T, Koike K, Ono M, Makino Y, Itagaki Y, Tanimoto M *et al.* (1996). Role of the human Y box-binding protein YB-1 in cellular sensitivity to the DNA-damaging agents cisplatin, mitomycin C, and ultraviolet light. *Cancer Res* **56**: 4224–4228.

Ohga T, Uchiumi T, Makino Y, Koike K, Wada M, Kuwano M *et al.* (1998). Direct involvement of the Y-box binding protein YB-1 in genotoxic stress-induced activation of the human multidrug resistance 1 gene. *J Biol Chem* **273**: 5997–6000.

Porcile C, Bajetto A, Barbieri F, Barbero S, Bonavia R, Biglieri M *et al.* (2005). Stromal cell-derived factor-1alpha (SDF-1alpha/CXCL12) stimulates ovarian cancer cell growth through the EGF receptor transactivation. *Exp Cell Res* **308**: 241–253.

Robledo MM, Bartolome RA, Longo N, Rodriguez-Frade JM, Mellado M, Longo I *et al.* (2001). Expression of functional chemokine receptors CXCR3 and CXCR4 on human melanoma cells. *J Biol Chem* **276**: 45098–45105.

Scotton CJ, Wilson JL, Milliken D, Stamp G, Balkwill FR. (2001). Epithelial cancer cell migration: a role for chemokine receptors? *Cancer Res* **61**: 4961–4965.

Scotton CJ, Wilson JL, Scott K, Stamp G, Wilbanks GD, Fricker S *et al.* (2002). Multiple actions of the chemokine CXCL12 on epithelial tumor cells in human ovarian cancer. *Cancer Res* **62**: 5930–5938.

Sorokin AV, Selyutina AA, Skabkin MA, Guryanov SG, Nazimov IV, Richard C *et al.* (2005). Proteasome-mediated cleavage of the Y-box-binding protein 1 is linked to DNA-damage stress response. *EMBO J* **24**: 3602–3612.

Stein U, Bergmann S, Scheffer GL, Scheper RJ, Royer HD, Schlag PM *et al.* (2005). YB-1 facilitates basal and 5-fluorouracil-inducible expression of the human major vault protein (MVP) gene. *Oncogene* **24**: 3606–3618.

Stein U, Jurchott K, Walther W, Bergmann S, Schlag PM, Royer HD. (2001). Hyperthermia-induced nuclear translocation of transcription factor YB-1 leads to enhanced expression of multidrug resistance-related ABC transporters. *J Biol Chem* **276**: 28562–28569.

Stenina OI, Poptic EJ, DiCorleto PE. (2000). Thrombin activates a Y box-binding protein (DNA-binding protein B) in endothelial cells. *J Clin Invest* **106**: 579–587.

Sutherland BW, Kucab J, Wu J, Lee C, Cheang MC, Yorida E *et al.* (2005). Akt phosphorylates the Y-box binding protein 1 at Ser102 located in the cold shock domain and affects the anchorage-independent growth of breast cancer cells. *Oncogene* **24**: 4281–4292.

Supplementary Information accompanies the paper on the Oncogene website (http://www.nature.com/onc).

Growth Stimulation of Non–Small Cell Lung Cancer Cell Lines by Antibody against Epidermal Growth Factor Receptor Promoting Formation of ErbB2/ErbB3 Heterodimers

Mari Maegawa,[1] Kenji Takeuchi,[1] Eishi Funakoshi,[1] Katsumi Kawasaki,[1] Kazuto Nishio,[2] Nobuyoshi Shimizu,[3] and Fumiaki Ito[1]

[1]Department of Biochemistry, Setsunan University; [2]Department of Genome Biology, Kinki University School of Medicine, Osaka, Japan; and [3]Department of Molecular Biology, Keio University School of Medicine, Tokyo, Japan

Abstract

Antibodies are the most rapidly expanding class of human therapeutics, including their use in cancer therapy. Monoclonal antibodies (mAb) against epidermal growth factor (EGF) receptor (EGFR) generated for cancer therapy block the binding of ligand to various EGFR-expressing human cancer cell lines and abolish ligand-dependent cell proliferation. In this study, we show that our mAb against EGFRs, designated as B4G7, exhibited a growth-stimulatory effect on various human cancer cell lines including PC-14, a non–small cell lung cancer cell line; although EGF exerted no growth-stimulatory activity toward these cell lines. Tyrosine phosphorylation of EGFRs occurred after treatment of PC-14 cells with B4G7 mAb, and it was completely inhibited by AG1478, a specific inhibitor of EGFR tyrosine kinase. However, this inhibitor did not affect the B4G7-stimulated cell growth, indicating that the growth stimulation by B4G7 mAb seems to be independent of the activation of EGFR tyrosine kinase. Immunoprecipitation with anti-ErbB3 antibody revealed that B4G7, but not EGF, stimulated heterodimerization between ErbB2 and ErbB3. ErbB3 was tyrosine phosphorylated in the presence of B4G7 but not in the presence of EGF. Further, the phosphorylation and B4G7-induced increase in cell growth were inhibited by AG825, a specific inhibitor of ErbB2. These results show that the ErbB2/ErbB3 dimer functions to promote cell growth in B4G7-treated cells. Changes in receptor-receptor interactions between ErbB family members after inhibition of one of its members are of potential importance in optimizing current EGFR family–directed therapies for cancer.

(Mol Cancer Res 2007;5(4):393–401)

Introduction

The epidermal growth factor (EGF) receptor (EGFR) is a member of the structurally related ErbB family of receptor tyrosine kinase. The ErbB family includes four members [i.e., EGFR (ErbB1), ErbB2, ErbB3, and ErbB4], all of which can dimerize with each other; in addition to homodimerization, specific ligands also induce heterodimerization of different pairs of the ErbB family members (1, 2). Although structural similarity exists between the family members, important differences are also present. Unlike the rest of the ErbB family, ErbB3 lacks tyrosine kinase activity (3, 4) and ErbB2 has no known ligand (5). EGF and transforming growth factor α bind directly only to EGFR, whereas neuregulins (also known as heregulins) are specific for ErbB3 and ErbB4 (6-8). Because expression levels of the family members and their ligands vary considerably in various cells, signaling pathways via activation of EGFR family members are complex.

Ligand-induced dimerization of EGFR is required to elevate its tyrosine kinase activity. The activated EGFR autophosphorylates tyrosine residues in its own COOH terminus, after which the receptor recruits and phosphorylates several signaling molecules such as growth factor receptor binding protein 2 (Grb-2), phospholipase Cγ, Src homology and collagen protein (Shc), and Grb2-associated binding protein 1 (Gab1; refs. 9, 10). Thus, ligands for EGFR are able to activate a variety of signaling pathways through their association with these signaling molecules. The mitogen-activated protein kinase (MAPK) pathway leading to phosphorylation of extracellular signal–regulated kinase (ERK)-1/2 plays an essential role in cell growth (9), and the phosphatidylinositol 3-kinase pathway is also important for cell growth and cell survival (11, 12). Another important signaling pathway is one for down-regulation of activated receptors. EGF binding is believed to result in localization of EGFR to clathrin-coated pits, from where EGFR is endocytosed. Recruitment of the Grb2/Casitas B-lineage lymphoma (Cbl) complex to the EGFR and subsequent activation of Cbl–dependent ubiquitination are essential for the delivery of EGFRs into these clathrin-coated pits (13).

Received 9/18/06; revised 1/16/07; accepted 2/6/07.
Grant support: Grant-in-Aid for Scientific Research from Japan Society for the Promotion of Science; fund for "Research for the Future" Program from the Japan Society for the Promotion of Science and Ministry of Education, Culture, Sports, Science, and Technology; and funding from the Fugaku Trust for Medical Research.
The costs of publication of this article were defrayed in part by the payment of page charges. This article must therefore be hereby marked *advertisement* in accordance with 18 U.S.C. Section 1734 solely to indicate this fact.
Note: M. Maegawa and K. Takeuchi contributed equally to this work.
Requests for reprints: Fumiaki Ito, Department of Biochemistry, Faculty of Pharmaceutical Sciences, Setsunan University, 45-1 Nagaotoge-cho, Hirakata, Osaka 573-0101, Japan. Phone: 81-72-866-3115; Fax: 81-72-866-3117. E-mail: fito@pharm.setsunan.ac.jp

doi:10.1158/1541-7786.MCR-06-0303

Alterations resulting in enhanced EGFR expression or function have been documented in a variety of tumors, including non–small cell lung cancer, breast cancer, and gliomas (14-17). These changes can occur due to increased production of ligands such as EGF and transforming growth factor α, increased gene transcription or amplification of EGFR, and receptor mutations resulting in constitutive activation of the receptor tyrosine kinase (18, 19). A variety of approaches to block the EGFR-mediated signaling pathway are currently undergoing clinical evaluation, including the use of anti-EGFR monoclonal antibodies (mAb), low molecular weight tyrosine kinase inhibitors, and immunoconjugates (20, 21). A series of anti-EGFR mAbs produced showed inhibitory activity toward the binding of EGF to A431 cells (22). As a result of the inhibition of receptor kinase, these anti-EGFR mAbs prevented ligand-induced stimulation of growth in a variety of cells that expressed both EGFR and ligand (20). It was also reported that anti-EGFR mAbs have the capacity to form receptor-containing complexes that result in receptor internalization, an important mechanism for attenuating receptor signaling (23).

It is important to further explore the primary mechanism by which various antibodies against EGFR affect growth of a variety of cells. In this present study, we decided to examine the growth-inhibitory effect of a mouse anti-human EGFR mAb, B4G7, which had previously been prepared against human A431 cells (24). Contrary to our expectations, B4G7 actually exhibited a growth-stimulatory effect in a variety of cells including gefitinib-sensitive and gefitinib-resistant non–small cell lung cancer cell lines, PC-9 and PC-14, respectively. Because EGF showed no stimulatory effect on the growth of these cell lines, we studied the molecular effects of B4G7 mAb and EGF in more detail. Our results indicate that mAb against EGFR increased growth of several cancer cell lines by stimulating the formation of ErbB2/ErbB3 heterodimers. Therefore, it is of importance to consider the status of all ErbB family members in cancer cells, not just the EGFR, for optimizing EGFR-directed cancer therapies.

Results

Growth-Stimulatory Activity of mAb against EGFR

We previously produced a mouse anti-human EGFR mAb against A431 cells and referred to it as B4G7 (24). In this study, we first examined the effect of the B4G7 mAb on the growth of various human cancer cell lines. The mAb exhibited a growth-stimulatory effect on human non–small cell lung cancer cell lines (PC-9, PC-14, and A549) as well as on A431 human epidermoid carcinoma cells, as determined from the results of a colorimetric assay (Fig. 1). The growth-stimulatory action of B4G7 was confirmed by counting the number of PC-14 cells in the presence or absence of B4G7 (data not shown). We also examined the mitogenic activity of purified mouse immunoglobulin G (IgG) toward PC-14 cells and found that their growth was not affected by this control IgG (data not shown). These were unexpected results because many research groups have previously reported that anti-EGFR mAbs block the binding of ligand to various EGFR-expressing human cancer cell lines and thereby abolish ligand-dependent cell proliferation (20). Because EGF showed no stimulatory effect on the growth of these cell lines, we next studied the molecular effects of B4G7 mAb and EGF on EGFR.

B4G7 mAb Affects Neither the Internalization nor the Down-Regulation of EGFR in PC-14 Cells

As shown in Fig. 2A, the majority of EGFRs were localized at the cell surface in the control cells. After EGF stimulation, the distribution of EGFRs was quite distinct: the cell-surface receptors disappeared; and EGFR-containing vesicles appeared in their place, thus indicating the internalization of EGFR on

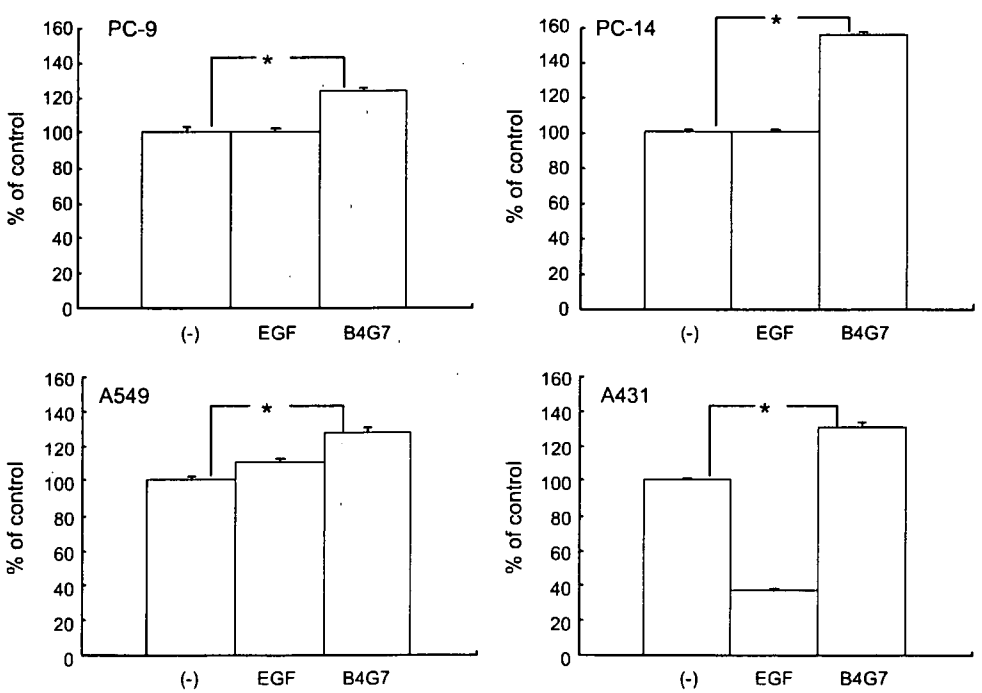

FIGURE 1. Growth-stimulatory effect of anti-EGFR mAb. Cells were treated or not with 100 ng/mL EGF or 10 μg/mL B4G7 for 2 d and their growth was estimated by means of WST-1 assay as described in Materials and Methods. Columns, mean (n = 6); bars, SD. *, $P < 0.01$. Similar results were obtained from five independent experiments.

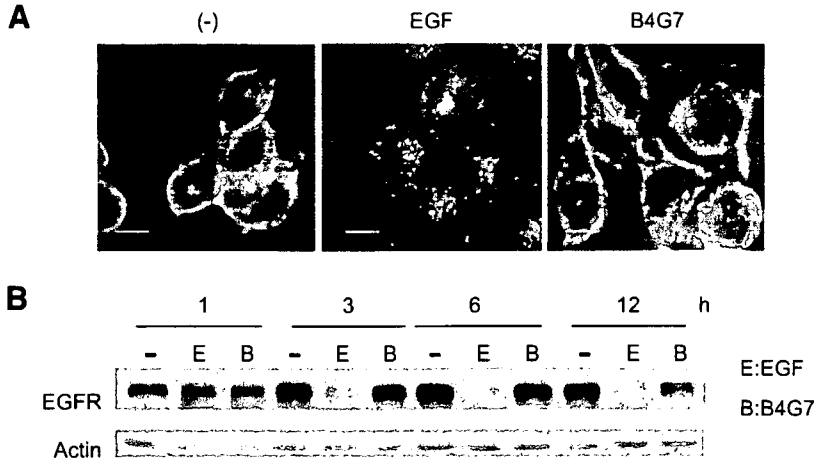

FIGURE 2. B4G7 affects neither the internalization nor the down-regulation of EGFR in PC-14 cells. **A.** PC-14 cells were treated with 100 ng/mL EGF or 10 μg/mL B4G7 mAb for 15 min. EGFR localization of these cells was determined by immunostaining as described in Materials and Methods. Bar, 10 μm. **B.** PC-14 cells were treated or not with EGF or B4G7 for the indicated times. Cell lysates were prepared and used for the detection of EGFR as described in Materials and Methods. The blot was reprobed with a β-actin antibody to show equal loading. Similar results were obtained from four independent experiments. Immunoblot analyses of total cellular lysates, which were prepared by using the Laemmli SDS buffer containing 5% mercaptoethanol, gave similar results.

EGF stimulation. In contrast, most of EGFRs still remained on the cell surface after B4G7 treatment. We next did Western blot analysis to assess the down-regulation of EGFRs after stimulation of PC-14 cells with EGF or B4G7 mAb (Fig. 2B). The down-regulation increased as the incubation time with EGF was lengthened, whereas EGFRs were still detected even 12 h after B4G7 treatment. Thus, B4G7 mAb affected neither the internalization nor the down-regulation of EGFRs.

Activation of EGFR, ERK1/2, and Akt after B4G7 Treatment

Next, we assessed EGFR phosphorylation on Tyr^{1173} and phosphorylation of ERK1/2 and Akt, downstream molecules of EGFR, after stimulation of PC-14 cells with EGF or B4G7 mAb (Fig. 3). Following the addition of EGF or B4G7, tyrosine phosphorylation of EGFR was observed with a peak at 10 to 15 min. ERK1/2 and Akt were phosphorylated even in the absence of EGF or B4G7, and this phosphorylation was further augmented in both EGF- and B4G7-treated cells. It thus seems that the growth-stimulatory activity of B4G7 mAb is not simply explained by its activity to stimulate tyrosine phosphorylation of EGFR and subsequent phosphorylation of ERK1/2 and Akt molecules. Figure 3 also shows the effect of AG1478, a specific inhibitor of EGFR tyrosine kinase, on tyrosine phosphorylation of EGFR. This inhibitor suppressed the tyrosine phosphorylation of EGFR in both EGF- and B4G7-treated cells, although a

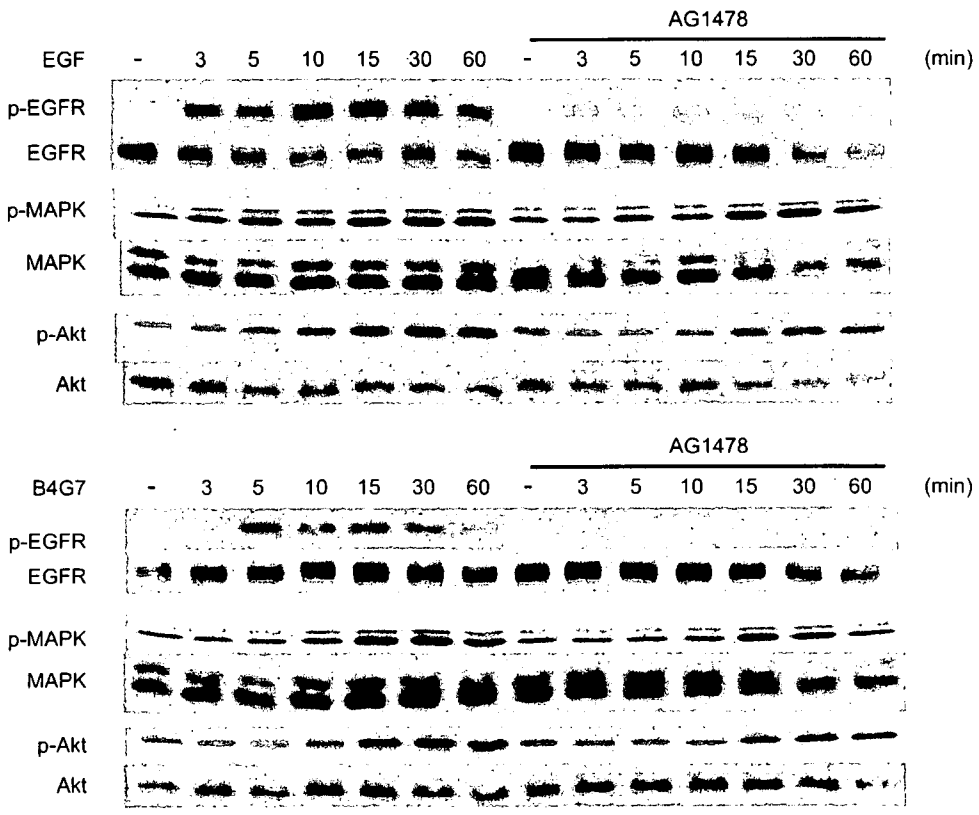

FIGURE 3. AG1478 inhibits tyrosine phosphorylation of EGFR but not phosphorylation of Akt and ERK1/2. PC-14 cells were pretreated with 200 nmol/L AG1478 for 2 h and then incubated with EGF or B4G7 for the indicated times. Total cell extracts were then prepared and electrophoresed on 7.5% SDS-PAGE for the detection of EGFR phosphorylation or on 12.5% SDS-PAGE for the detection of phosphorylated ERK1/2 and phosphorylated Akt. EGFR, ERK1/2, and Akt and phosphorylation of these molecules were detected by using each corresponding antibody. Similar results were obtained from three independent experiments.

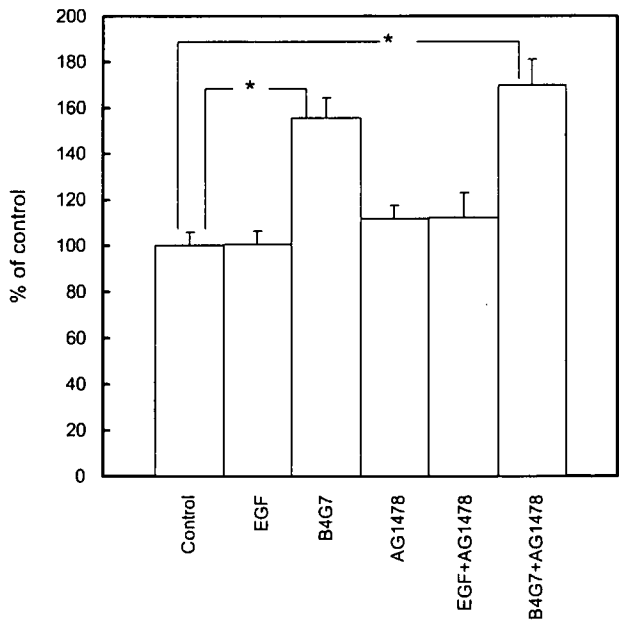

FIGURE 4. AG1478 shows no inhibitory activity against B4G7-stimulated cell growth. PC-14 cells were pretreated with 200 nmol/L AG1478 for 2 h and then incubated with 100 ng/mL EGF or 10 μg/mL B4G7. After 2 d of incubation, their growth was estimated by means of the WST-1 assay as described in Materials and Methods. Columns, mean (n = 6); bars, SD. *, $P < 0.01$. Similar results were obtained from three independent experiments.

faint band of phosphorylated EGFR band was still visible in EGF-treated cells after AG1478 treatment. On the other hand, the inhibitory activity of the inhibitor against the phosphorylation of ERK1/2 and Akt was not remarkable. This result suggests that activation of the two signaling proteins ERK1/2 and Akt in B4G7-treated cells occurred via a pathway independent of the tyrosine phosphorylation of EGFR.

Next, we determined the effect of AG1478 on the B4G7-stimulated cell growth (Fig. 4). This inhibitor showed no inhibitory activity against the stimulation of PC-14 cell growth, indicating that the growth stimulation by B4G7 mAb seems to have been independent of the activation of EGFR tyrosine kinase.

Stimulated Formation of HER2/HER3 Heterodimer by B4G7

EGFR, ErbB2, ErbB3, and ErbB4 are members of the ErbB family of receptors. ErbB receptors signal through a network involving receptor homodimerization and heterodimerization. Thus, we examined whether B4G7 mAb would cause the down-regulation of other members of the ErbB family although it did not down-regulate EGFR. As shown in Fig. 5A, incubation of PC-14 cells with EGF, but not with B4G7 mAb, caused down-regulation of ErbB2. On the other hand, neither EGF nor B4G7 mAb down-regulated ErbB3. Many studies have shown that ligand-activated EGFRs preferentially recruit ErbB2 into a heterodimeric complex in cells that coexpress ErbB2 (25). Thus, it is most likely that EGF down-regulated ErbB2 through the increased formation of EGFR/ErbB2 heterodimer. In fact, when lysates from EGF-treated PC-14 cells were incubated with anti-EGFR antibody, ErbB2 became detectable in the immunocomplex (Fig. 5B). In contrast, it was not detected in lysates from B4G7-treated PC-14 cells.

ErbB3 has been observed to preferentially heterodimerize with ErbB2 in several cancers, leading to a strong oncogenic signal thought to promote tumor cell proliferation (26). We thus studied whether treatment of PC-14 cells with EGF or B4G7 would affect complex formation between ErbB2 and ErbB3. Immunoprecipitation with anti-ErbB3 antibody revealed that

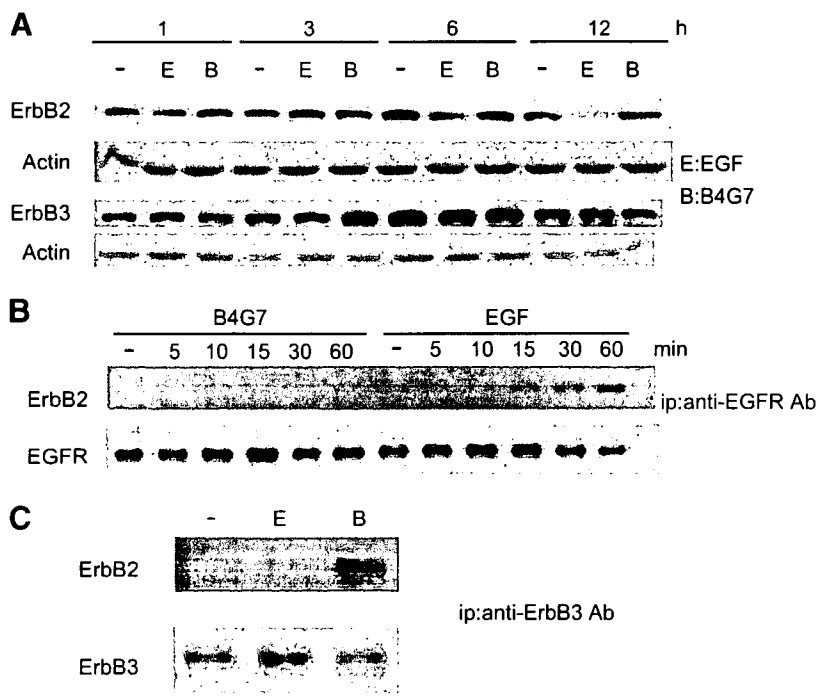

FIGURE 5. B4G7 stimulates ErbB2/ErbB3 heterodimer formation. **A.** PC-14 cells were treated or not with EGF or B4G7 for the indicated times. Lysates were prepared from these cells and used for the detection of ErbB2 and ErbB3 as described in Materials and Methods. The blot was reprobed with a β-actin antibody to show equal loading. **B.** EGFR was immunoprecipitated from the lysates by using anti-EGFR antibody, and the immunoprecipitates were examined for EGFR and ErbB2 as described in Materials and Methods. **C.** PC-14 cells were treated or not with EGF or B4G7 for 15 min. The supernatant fractions of cell lysates were immunoprecipitated with anti-c-erbB3 antibody, and proteins eluted from the immunocomplexes were subjected to SDS-PAGE and used for immunoblot analysis of ErbB2 and ErbB3. Similar results were obtained from three independent experiments.

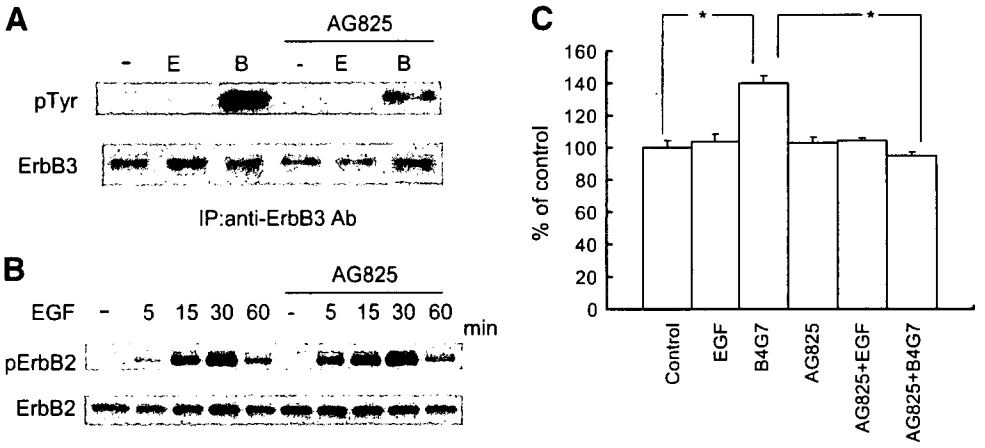

FIGURE 6. AG825 inhibits tyrosine phosphorylation of ErbB3 and cell growth in B4G7-treated cells. **A.** PC-14 cells were pretreated with 0.5 μmol/L AG825 for 2 h and then treated with EGF or B4G7 for 15 min. The cells were then subjected to immunoprecipitation with anti–c-erbB3 antibody and used for the detection of ErbB3 and its tyrosine phosphorylated form by using anti-ErbB3 antibody and anti-phosphotyrosine antibody (PY20). **B.** PC-14 cells were incubated with EGF for the indicated times after AG825 (0.5 μmol/L) pretreatment. Cell lysates were then prepared and used for immunoblot analysis of ErbB2 and its phosphorylation by using anti–c-ErbB2 antibody and anti–phospho-erbB2 (Tyr^{1248}) antibody, respectively. **C.** PC-14 cells were incubated with EGF or B4G7 for 2 d in the presence of 0.5 μmol/L AG825. Their growth was estimated by means of the WST-1 assay as described in Materials and Methods. Columns, mean (n = 6); bars, SD. *, $P < 0.01$. Similar results were obtained from three independent experiments.

B4G7 but not EGF stimulated heterodimeriztion between ErbB2 and ErbB3 (Fig. 5C).

The EGFR extracellular domain (amino acids 1-621) shares 45% amino acid identity with that of ErbB3. Due to this homology, specific B4G7 antibody against EGFR may show some cross-reactivity against ErbB3. We thus determined whether B4G7 binds to ErbB3 as well as to EGFR. Immunocomplexes were prepared from lysates of PC-14 cells using B4G7 and assayed for the presence of ErbB3 by immunoblot analysis. Because ErbB3 was not detected at all in these complexes (data not shown), B4G7 seems to promote formation of ErbB2/ErbB3 heterodimers by its binding to EGFR but not to ErbB3.

B4G7-Stimulated Cell Growth Requires ErbB2/ErbB3 Heterodimer and ErbB3 Tyrosine Phosphorylation

If ErbB2/ErbB3 heterodimers are formed in the presence of B4G7, ErbB3 of B4G7-treated cells could be phosphorylated by ErbB2 tyrosine kinase. Indeed, ErbB3 was tyrosine phosphorylated in the presence of B4G7 but not in the presence of EGF (Fig. 6A). Further, this phosphorylation was inhibited by AG825, a specific inhibitor of ErbB2. On the contrary, EGF-induced phosphorylation of ErbB2 at Tyr^{1248}, possibly through heterodimerization of EGFR/ErbB2, was not inhibited by AG825 (Fig. 6B), indicating a selective inhibitory action of this inhibitor against ErbB2 tyrosine kinase. Further analysis of immunocomplexes formed in the presence of anti-EGFR antibody confirmed that ErbB2 phosphorylation by EGFR tyrosine kinase was not inhibited by this inhibitor: tyrosine-phosphorylated ErbB2 was detected only in the immunocomplexes from EGF-treated cells but not in those from B4G7-treated cells, and this phosphorylation was not inhibited by AG825 (data not shown).

To examine association of ErbB2 tyrosine kinase with B4G7-induced cell growth, we treated PC-14 cells with AG825 before their stimulation with EGF or B4G7. As shown in Fig. 6C, cell growth increased by B4G7 was suppressed to the control level by this pretreatment. These results show that ErbB2 tyrosine kinase and the ErbB2/ErbB3 dimer function to promote cell growth in B4G7-treated cells.

Discussion

We previously produced a mAb against EGFRs by immunizing BALB/c mice with human epidermoid carcinoma A431 cells (24). This mAb, which we named B4G7, inhibited the binding of ^{125}I-EGF to A431 cells and human fibroblasts and specifically precipitated EGFR of A431 cells. Sato et al. (22) also produced mAbs against A431 cells and found that these antibodies were capable of inhibiting both the binding of EGF to its receptor and ligand-induced cell proliferation. In this study, we made the unexpected finding that B4G7 mAb exerted growth-stimulatory activity toward various cancer cell lines. We initially thought that B4G7 stimulated cell growth via signaling pathways originating from EGFR tyrosine phosphorylation because B4G7 stimulated EGFR tyrosine phosphorylation and also phosphorylation of MAPK and Akt, two downstream signaling molecules of EGFR. However, the growth stimulation by B4G7 was independent of EGFR activation itself because the stimulation was not affected by the presence of AG1478, an EGFR tyrosine kinase–specific inhibitor.

EGFR forms homodimers as well as heterodimers with the other ErbB family members, and cooperation between ErbB family members plays pivotal roles in a variety of critical functions. It is thus reasonable to speculate that binding of B4G7 mAb to EGFR affects cross-talk among the ErbB family and the cellular effects mediated by these receptors. In B4G7-treated PC-14 cells, the EGFR/ErbB2 complex was not detected, although its formation was increased in response to EGF (Fig. 5B). Therefore, B4G7 may have blocked the ability of EGFR to heterodimerize with ErbB2 or ErbB3 and thus facilitated enhanced dimerization between ErbB2 and ErbB3. In fact, ErbB2/ErbB3 heterodimers were formed in the presence of

B4G7 but not in the presence of EGF (Fig. 5C). In EGF-treated PC-14 cells, major combinations of ErbB family members were EGFR homodimer and EGFR/ErbB2 heterodimer. AG1478 inhibited, but not completely, EGFR phosphorylation, whereas it inhibited phosphorylation of ERK1/2 and Akt to a lesser extent. The limited efficacy of AG1478 could have arisen from unblocked ErbB2 signaling in the form of EGFR/ErbB2.

At least six different ligands are known to bind to EGFR. These ligands include EGF, transforming growth factor α, amphiregulin, heparin-binding EGF, betacellulin, and epiregulin (1, 20, 27). A second class of ligands, collectively termed neuregulin, bind directly to ErbB3 and/or ErbB4 (6-8). It is known that ErbB2 and ErbB3 dimerize to produce a high-affinity receptor for neuregulin-1. Because production and secretion of neuregulin-1 have been reported in many human lung cancer cell lines (28), it is very likely that neuregulin-1 or neuregulin isoform is secreted from PC-14 cells and thereafter activates the ErbB2/ErbB3 heterodimer in an autocrine fashion. This likelihood is supported by the finding that ErbB3 phosphorylation was increased on B4G7 addition and abrogated in the presence of AG825, which selectively inhibits the ErbB2 kinase activity.

The physiologic role of ErbB2, in the context of ErbB ligand signaling, is to serve as a coreceptor (29, 30). ErbB2 seems to be the preferred partner of the other ligand-bound ErbBs (25, 31). ErbB3 functions as an indispensable ErbB2 dimerization partner and is required for proliferation of ErbB2-overexpressing tumor cells, and neither ErbB1 nor ErbB4 could replace ErbB3 as partner of ErbB2 to drive proliferation. Therefore, it seems that the ErbB2/ErbB3 formed in the presence of B4G7 but not in the presence of EGF transmits effective proliferation signals in PC-14 cells. This notion is supported by our finding that AG825, a specific inhibitor of ErbB2, suppressed B4G7-stimulated cell growth (Fig. 6C). Taken together, these findings indicate that B4G7 transmitted signals for growth stimulation by increasing the formation of ErbB2/ErbB3 (see Fig. 7).

The signals generated by activated growth factor receptors are generally attenuated by the process of receptor internalization, which leads to receptor degradation (32, 33). Neuregulin has been reported to undergo slow endocytosis followed by receptor recycling to the plasma membrane (34). In contrast, most of the EGF-stimulated EGFR molecules are destined to lysosomal degradation. Due to the consequent clearance of EGFR but not ErbB3 molecules from the cell surface, the mitogenic signal evoked by EGF is less potent than the neuregulin signal (29). In PC-14 cells, EGFR and ErbB2 were down-regulated in the presence of EGF, but their levels were unchanged after B4G7 treatment. Therefore, slow endocytosis and receptor recycling of ErbB2 and ErbB3 may explain the capacity of B4G7 to deliver more sustained mitogenic signals than EGF. Another mechanism for the different mitogenic capacity probably involves the recruitment of distinct sets of downstream effectors to each of the activated ErbB family members. One of the downstream effectors is phosphatidylinositol 3-kinase, the activation of which results in the phosphorylation of the 3′ position of phosphatidylinositol 4,5-bis-phosphate to yield phosphatidylinositol 3,4,5-tris-phosphate. Phosphatidylinositol 3,4,5-tris-phosphate, in turn, activates several downstream signaling molecules including Akt. ErbB3 effectively couples to the phosphatidylinositol 3-kinase/Akt pathway because it has six tyrosine phosphorylation sites with YXXMs motifs, which serve as excellent binding sites for phosphatidylinositol 3-kinase (35, 36). Because the phosphatidylinositol 3-kinase/Akt pathway originating from ErbB3 is suggested to play an important role in the stimulation of cell growth (37, 38), it is reasonable to speculate that this pathway is linked to the mitogenic superiority of ErbB3. In this study, we determined the phosphorylation time course of Akt in B4G7- and EGF-treated cells, but there was no significant difference between their phosphorylation kinetics.

Neuregulin activates ERK MAPK, a signaling pathway that is critical in the mitogenic effect of neuregulin (39, 40). It has been indicated that sustained, but not transient, activation of ERK induces phosphorylation of immediate early gene products, which leads to their stabilization and activation, resulting in appropriate gene expression, such as that of cyclin D (41, 42). Further, only sustained ERK activation induces and maintains decreased expression levels of antiproliferative genes (43). Thus, the duration and magnitude of ERK activity is a key determinant for the mitogenic response of various cells to EGF (44, 45). The differential mitogenic response of PC-14 cells to

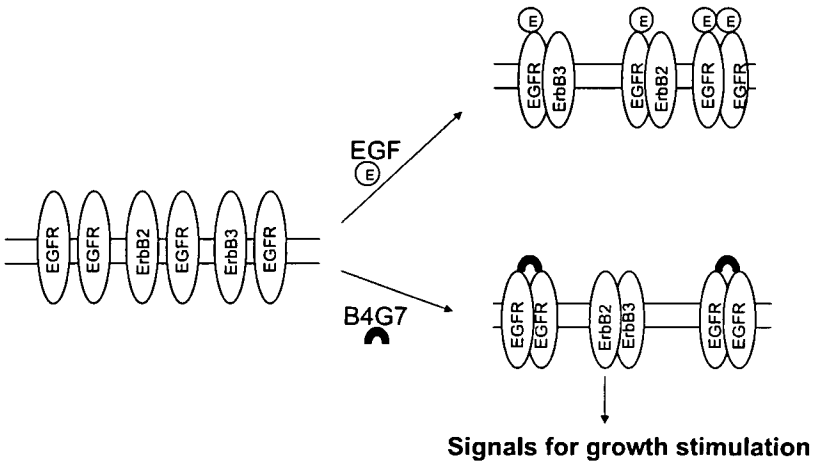

FIGURE 7. Schematic representation of how mAb B4G7 stimulates cell growth. Homodimers and heterodimers of EGFR are formed on EGF addition. On the other hand, the ErbB2/ErbB3 heterodimer is formed in the presence of B4G7 mAb because binding of B4G7 mAb to EGFR inhibits the ability of EGFR to form heterodimers with ErbB2 and ErbB3. ErbB2/ErbB3, unlike EGFR dimers, continues to exist on the cell surface and transmits signals for growth stimulation. ErbB2/ErbB3 may be activated in an autocrine fashion.

EGF and B4G7 may be related to the differential kinetics of ERK activation in B4G7- and EGF-treated cells. However, both EGF and B4G7 mAb stimulated phosphorylation of ERK in a similar time-dependent manner (see Fig. 3). We studied phosphorylation of ERK and Akt in PC-14 cells treated with EGF or B4G7 for a longer period of time, but observed no significant difference in the phosphorylation time course between B4G7- and EGF-treated cells.[4] The duration of Akt and MAPK activities may be essential, but not sufficient, for ensuring G_1 phase progression of PC-14 cells. A more detailed side-by-side comparison of PC-14 cells treated with EGF or B4G7 should provide a hint for elucidating the signaling pathway for B4G7-induced cell growth.

A variety of approaches to block the EGFR-mediated signaling pathway are undergoing clinical evaluation, including the use of mAbs against EGFR and ErbB2 (46). The study presented here might have important clinical implications because it indicates that mAb against EGFR stimulated the growth of several cancer cell lines by affecting dimerization of EGFR family members other than EGFR. Similarly, ZD1839, a specific EGFR tyrosine kinase inhibitor, has been reported to inhibit the growth of ErbB2-overexpressing breast cancer cells, possibly by sequestration of ErbB2 and ErbB3 receptors in an inactive heterodimer configuration with EGFR (47). Another group also reported that elimination of ErbB2 signaling resulted in an increase in EGFR expression and activation and that its increased activation contributed to sustained cell survival (48). Changes in receptor-receptor interactions between ErbB family members and compensatory changes in the ErbB family after inhibition of one of its members are of potential importance in optimizing current EGFR family–directed therapies for cancer.

Materials and Methods

Materials

EGF (ultrapure) from mouse submaxillary glands was purchased from Toyobo Co. Ltd. (Osaka, Japan). FCS, phenylmethylsulfonyl fluoride, pepstatin A, *p*-toluenesulfonyl-L-arginine methyl ester, leupeptin, and aprotinin came from Sigma (St. Louis, MO). AG1478 [4-(3-chloroanilino)-6,7-dimethoxyquinazoline] and AG825 [4-hydroxy-3-methoxy-5-(benzothiazolylthiomethyl)benzylidenecyanoacetamide] were purchased from Calbiochem (San Diego, CA). RPMI 1640 and DMEM were from Nissui Pharmaceutical Co. Ltd. (Tokyo, Japan). Antibodies used and their sources were as follows: anti-phosphotyrosine (PY20; BD Transduction Laboratories, San Jose, CA); anti–phospho-EGFR (Tyr^{1173}) and anti–phospho-erbB2 (Tyr^{1248}) (Upstate Biotechnology, Lake Placid, NY); anti-EGFR (1005) and anti-ErbB3 (C-17; Santa Cruz Biotechnology, Inc., Santa Cruz, CA); anti-Akt (Cell Signaling Technology, Inc., Beverly, MA); anti-MAPK (Sigma); anti–phospho-Akt (Tyr^{473}) and anti-ACTIVE MAPK (Promega, Madison, WI); anti–c-ErbB2/c-Neu (Ab-3; Calbiochem); horseradish peroxidase–conjugated swine anti-rabbit immunoglobulin (DAKO, Glostrup, Denmark); and horseradish peroxidase–linked sheep anti-mouse IgG and biotinylated sheep anti-mouse immunoglobulin (GE Healthcare, Piscataway, NJ). A mouse anti-human EGFR mAb (B4G7) was purified from mouse ascites by ammonium sulfate precipitation and protein G column chromatography. All other chemicals were commercial products of reagent grade.

Cell Culture

Human non–small cell lung cancer cell lines PC-9 and PC-14 were obtained from Tokyo Medical University (Tokyo, Japan). Both lines were cultured in RPMI 1640 supplemented with 5% FCS in 5% CO_2 at 37°C in a fully humidified atmosphere. Human adenocarcinoma A549 and epidermoid carcinoma A431 were cultured in DMEM supplemented with 5% FCS. Exponentially growing cells were used in all experiments.

Growth Stimulation Assay

Cells were seeded at a density of 2×10^3 per well into a 96-well microtiter plate and cultured for 2 days in the presence of 5% FCS. They were then treated with 100 ng/mL EGF or 10 μg/mL B4G7 mAb. After incubation for 48 h, growth stimulation was quantified by a colorimetric assay with the WST-1 reagent according to the manufacturer's instruction (Dojindo Laboratories, Kumamoto, Japan).

Preparation of Cellular Lysates and Immunoblotting

PC-14 cells were seeded at a density of 1.2×10^5 per 35-mm-diameter dish and cultured for 2 days. They were then treated or not with 100 ng/mL EGF or 10 μg/mL B4G7 mAb for indicated times at 37°C. When the effects of AG1478 or AG825 were assayed, these inhibitors were added 2 h before the addition of EGF or B4G7. The cells were then washed with ice-cold PBS and subsequently lysed by incubating in hypotonic buffer [10 mmol/L Tris-HCl (pH 7.8), containing 10 mmol/L NaCl, 1.5 mmol/L $MgCl_2$, 0.5 mmol/L DTT, 0.5 mmol/L phenylmethylsulfonyl fluoride, 2 μg/mL leupeptin, 2 μg/mL aprotinin, and 0.3% NP40]. The lysates were incubated on ice for 10 min and clarified by centrifugation at $1,500 \times g$ for 5 min at 4°C. Total proteins (10 μg/mL) from the supernatant fractions were resolved by SDS-PAGE and transferred to Immobilon-P membrane (Millipore, Bedford, MA). The membranes were sequentially incubated, first with primary antibody for 2 h and then with horseradish peroxidase–conjugated anti-rabbit IgG antibody (1:1,000) or anti-mouse IgG antibody (1:1,000) for 1 h. Finally, the proteins were visualized by use of an enhanced chemiluminescence Western Blotting Detection System (GE Healthcare) and exposed to autoradiography film (Fuji Medical X-ray film RX-U, Fuji Photo Film Co., Ltd., Tokyo, Japan).

Immunostaining of Cells for Confocal Laser Scanning Microscopic Observation

Immunostaining of cells was done as previously described (49). Briefly, PC-14 cells were grown on coverslips for 2 days and then stimulated with 100 ng/mL EGF or 10 μg/mL B4G7 mAb for 15 min. The cells were fixed with methanol for 5 min at −20°C, after which they were washed thrice with 20 mmol/L TBS (pH 7.4) containing 1 mmol/L $CaCl_2$ (TBS-Ca) and incubated with anti-EGFR antibody for 2 h at room temperature.

[4] Kenji Takenchi and Fumiaki Ito, unpublished data.

After being washed with TBS-Ca, the cells were incubated with biotinylated sheep anti-mouse immunoglobulin antibody (1:100) for 1 h at room temperature and then with Texas red–labeled streptavidin (GE Healthcare). The stained cells were observed under a confocal laser scanning microscope (MRC1024, Bio-Rad, Hercules, CA).

Immunoprecipitation

PC-14 cells were seeded at 1.2×10^6 per 150-mm dish and incubated in RPMI 1640/5% FCS for 2 days. The cultures were then incubated for 2 h in the presence or absence of 0.5 μmol/L AG825 and treated with either EGF or B4G7 for the indicated times at 37°C. They were lysed in hypotonic buffer and centrifuged at $1,500 \times g$ for 5 min as described above. The supernatant fractions were incubated overnight at 4°C with anti–c-erbB3 (clone 2F12) antibody (LabVision Co., Fremont, CA) or anti-EGFR antibody (B4G7). Immunocomplexes were collected on protein G-sepharose (GE Healthcare). Bound proteins were washed thrice with 10 mmol/L Tris-HCl buffer (pH 7.4) containing 135 mmol/L NaCl, 0.1% NP40, 0.1% Triton X-100, a cocktail of protease inhibitors (0.1 mg/mL phenylmethylsulfonyl fluoride, 2 μg/mL leupeptin, 1 μg/mL pepstatin A, 0.1 μg/mL *p*-toluenesulfonyl-L-arginine methyl ester), 1 mmol/L sodium orthovanadate, 2 mmol/L EGTA, 5 mmol/L EDTA, 50 mmol/L sodium fluoride, and 30 mmol/L $Na_4P_2O_7$ and once with TBS and eluted in Laemmli sample buffer containing 2-mercaptoethanol. Eluted proteins were subjected to SDS-PAGE and immunoblotted as described above.

Protein Assay

Protein content was assayed by using a Coomassie Plus Protein Assay reagent (Pierce Chemical Co., Rockford, IL) according to the manufacturer's instructions.

References

1. Olayioye MA, Neve RM, Lane HA, Hynes NE. The ErbB signaling network: receptor heterodimerization in development and cancer. EMBO J 2000;19:3159–67.

2. Yarden Y, Sliwkowski MX. Untangling the ErbB signalling network. Nat Rev Mol Cell Biol 2001;2:127–37.

3. Sliwkowski MX, Schaefer G, Akita RW, et al. Coexpression of erbB2 and erbB3 proteins reconstitutes a high affinity receptor for heregulin. J Biol Chem 1994;269:14661–5.

4. Guy PM, Platko JV, Cantley LC, Cerione RA, Carraway KL III. Insect cell-expressed p180erbB3 possesses an impaired tyrosine kinase activity. Proc Natl Acad Sci U S A 1994;91:8132–6.

5. Klapper LN, Glathe S, Vaisman N, et al. The ErbB-2/HER2 oncoprotein of human carcinomas may function solely as a shared coreceptor for multiple stroma-derived growth factors. Proc Natl Acad Sci U S A 1999;96:4995–5000.

6. Tzahar E, Levkowitz G, Karunagaran D, et al. ErbB-3 and ErbB-4 function as the respective low and high affinity receptors of all Neu differentiation factor/heregulin isoforms. J Biol Chem 1994;269:25226–33.

7. Lupu R, Colomer R, Kannan B, Lippman ME. Characterization of a growth factor that binds exclusively to the erbB-2 receptor and induces cellular responses. Proc Natl Acad Sci U S A 1992;89:2287–91.

8. Holmes WE, Sliwkowski MX, Akita RW, et al. Identification of heregulin, a specific activator of p185erbB2. Science 1992;256:1205–10.

9. Schlessinger J. Cell signaling by receptor tyrosine kinases. Cell 2000;103:211–25.

10. Ruff-Jamison S, McGlade J, Pawson T, Chen K, Cohen S. Epidermal growth factor stimulates the tyrosine phosphorylation of SHC in the mouse. J Biol Chem 1993;268:7610–2.

11. Marte BM, Downward J. PKB/Akt: connecting phosphoinositide 3-kinase to cell survival and beyond. Trends Biochem Sci 1997;22:355–8.

12. Takeuchi K, Ito F. Suppression of Adriamycin-induced apoptosis by sustained activation of the phosphatidylinositol-3′-OH kinase-Akt pathway. J Biol Chem 2004;279:892–900.

13. Stang E, Blystad FD, Kazazic M, et al. Cbl-dependent ubiquitination is required for progression of EGF receptors into clathrin-coated pits. Mol Biol Cell 2004;15:3591–604.

14. Lynch TJ, Bell DW, Sordella R, et al. Activating mutations in the epidermal growth factor receptor underlying responsiveness of non-small-cell lung cancer to gefitinib. N Engl J Med 2004;350:2129–39.

15. Arteaga CL. Epidermal growth factor receptor dependence in human tumors: more than just expression? Oncologist 2002;7(Suppl 4):31–9.

16. Humphrey PA, Gangarosa LM, Wong AJ, et al. Deletion-mutant epidermal growth factor receptor in human gliomas: effects of type II mutation on receptor function. Biochem Biophys Res Commun 1991;178:1413–20.

17. Wong AJ, Bigner SH, Bigner DD, Kinzler KW, Hamilton SR, Vogelstein B. Increased expression of the epidermal growth factor receptor gene in malignant gliomas is invariably associated with gene amplification. Proc Natl Acad Sci U S A 1987;84:6899–903.

18. Jorissen RN, Walker F, Pouliot N, Garrett TP, Ward CW, Burgess AW. Epidermal growth factor receptor: mechanisms of activation and signalling. Exp Cell Res 2003;284:31–53.

19. Chu CT, Everiss KD, Wikstrand CJ, Batra SK, Kung HJ, Bigner DD. Receptor dimerization is not a factor in the signalling activity of a transforming variant epidermal growth factor receptor (EGFRvIII). Biochem J 1997;324:855–61.

20. Mendelsohn J, Baselga J. The EGF receptor family as targets for cancer therapy. Oncogene 2000;19:6550–65.

21. Herbst RS, Onn A, Mendelsohn J. The role of growth factor signaling in malignancy. In: Frank DA, editor. Signal transduction in cancer. Boston/Dordrecht/London: Kluwer Academic Publishers; 2003. p. 19–72.

22. Sato JD, Kawamoto T, Le AD, Mendelsohn J, Polikoff J, Sato GH. Biological effects *in vitro* of monoclonal antibodies to human epidermal growth factor receptors. Mol Biol Med 1983;1:511–29.

23. Fan Z, Lu Y, Wu X, Mendelsohn J. Antibody-induced epidermal growth factor receptor dimerization mediates inhibition of autocrine proliferation of A431 squamous carcinoma cells. J Biol Chem 1994;269:27595–602.

24. Behzadian MA, Shimizu N. Monoclonal antibody that immunoreacts with a subclass of human receptors for epidermal growth factor. Cell Struct Funct 1985;10:219–32.

25. Graus-Porta D, Beerli RR, Daly JM, Hynes NE. ErbB-2, the preferred heterodimerization partner of all ErbB receptors, is a mediator of lateral signaling. EMBO J 1997;16:1647–55.

26. Holbro T, Beerli RR, Maurer F, Koziczak M, Barbas CF III, Hynes NE. The ErbB2/ErbB3 heterodimer functions as an oncogenic unit: ErbB2 requires ErbB3 to drive breast tumor cell proliferation. Proc Natl Acad Sci U S A 2003;100:8933–8.

27. Alroy I, Yarden Y. The ErbB signaling network in embryogenesis and oncogenesis: signal diversification through combinatorial ligand-receptor interactions. FEBS Lett 1997;410:83–6.

28. Gollamudi M, Nethery D, Liu J, Kern JA. Autocrine activation of ErbB2/ErbB3 receptor complex by NRG-1 in non-small cell lung cancer cell lines. Lung Cancer 2004;43:135–43.

29. Pinkas-Kramarski R, Soussan L, Waterman H, et al. Diversification of Neu differentiation factor and epidermal growth factor signaling by combinatorial receptor interactions. EMBO J 1996;15:2452–67.

30. Riese DJ II, van Raaij TM, Plowman GD, Andrews GC, Stern DF. The cellular response to neuregulins is governed by complex interactions of the erbB receptor family. Mol Cell Biol 1995;15:5770–6.

31. Tzahar E, Waterman H, Chen X, et al. A hierarchical network of interreceptor interactions determines signal transduction by Neu differentiation factor/neuregulin and epidermal growth factor. Mol Cell Biol 1996;16:5276–87.

32. Jaramillo ML, Leon Z, Grothe S, Paul-Roc B, Abulrob A, O'Connor McCourt M. Effect of the anti-receptor ligand-blocking 225 monoclonal antibody on EGF receptor endocytosis and sorting. Exp Cell Res 2006;312:2778–90.

33. Wiley HS. Trafficking of the ErbB receptors and its influence on signaling. Exp Cell Res 2003;284:78–88.

34. Waterman H, Sabanai I, Geiger B, Yarden Y. Alternative intracellular routing of ErbB receptors may determine signaling potency. J Biol Chem 1998;273:13819–27.

35. Ram TG, Ethier SP. Phosphatidylinositol 3-kinase recruitment by p185erbB-2

and erbB-3 is potently induced by neu differentiation factor/heregulin during mitogenesis and is constitutively elevated in growth factor-independent breast carcinoma cells with c-erbB-2 gene amplification. Cell Growth Differ 1996;7: 551–61.

36. Cantley LC, Auger KR, Carpenter C, et al. Oncogenes and signal transduction. Cell 1991;64:281–302.

37. Engelman JA, Janne PA, Mermel C, et al. ErbB-3 mediates phosphoinositide 3-kinase activity in gefitinib-sensitive non-small cell lung cancer cell lines. Proc Natl Acad Sci U S A 2005;102:3788–93.

38. Kim HH, Sierke SL, Koland JG. Epidermal growth factor-dependent association of phosphatidylinositol 3-kinase with the erbB3 gene product. J Biol Chem 1994;269:24747–55.

39. Fiddes RJ, Janes PW, Sivertsen SP, Sutherland RL, Musgrove EA, Daly RJ. Inhibition of the MAP kinase cascade blocks heregulin-induced cell cycle progression in T-47D human breast cancer cells. Oncogene 1998;16:2803–13.

40. Vijapurkar U, Kim MS, Koland JG. Roles of mitogen-activated protein kinase and phosphoinositide 3′-kinase in ErbB2/ErbB3 coreceptor-mediated heregulin signaling. Exp Cell Res 2003;284:291–302.

41. Murphy LO, Smith S, Chen RH, Fingar DC, Blenis J. Molecular interpretation of ERK signal duration by immediate early gene products. Nat Cell Biol 2002;4:556–64.

42. Weber JD, Raben DM, Phillips PJ, Baldassare JJ. Sustained activation of extracellular-signal-regulated kinase 1 (ERK1) is required for the continued expression of cyclin D1 in G_1 phase. Biochem J 1997;326:61–8.

43. Yamamoto T, Ebisuya M, Ashida F, Okamoto K, Yonehara S, Nishida E. Continuous ERK activation down-regulates antiproliferative genes throughout G_1 phase to allow cell-cycle progression. Curr Biol 2006;16:1171–82.

44. Meloche S, Seuwen K, Pages G, Pouyssegur J. Biphasic and synergistic activation of p44mapk (ERK1) by growth factors: correlation between late phase activation and mitogenicity. Mol Endocrinol 1992;6:845–54.

45. Torii S, Yamamoto T, Tsuchiya Y, Nishida E. ERK MAP kinase in G cell cycle progression and cancer. Cancer Sci 2006;97:697–702.

46. Carter P, Smith L, Ryan M. Identification and validation of cell surface antigens for antibody targeting in oncology. Endocr Relat Cancer 2004;11:659–87.

47. Anido J, Matar P, Albanell J, et al. ZD1839, a specific epidermal growth factor receptor (EGFR) tyrosine kinase inhibitor, induces the formation of inactive EGFR/HER2 and EGFR/HER3 heterodimers and prevents heregulin signaling in HER2-overexpressing breast cancer cells. Clin Cancer Res 2003;9:1274–83.

48. Hu YP, Venkateswarlu S, Sergina N, et al. Reorganization of ErbB family and cell survival signaling following knockdown of ErbB2 in colon cancer cells. J Biol Chem 2005;280:27383–92.

49. Funakoshi E, Hori T, Haraguchi T, et al. Overexpression of the human MNB/DYRK1A gene induces formation of multinucleate cells through overduplication of the centrosome. BMC Cell Biol 2003;4:12.

Jpn J Clin Oncol 2007;37(5)329–336
doi:10.1093/jjco/hym035

Review Article

Genes Regulating the Sensitivity of Solid Tumor Cell Lines to Cytotoxic Agents: A Literature Review

Ikuo Sekine[1], John D. Minna[2], Kazuto Nishio[3], Nagahiro Saijo[4] and Tomohide Tamura[1]

[1]Division of Internal Medicine and Thoracic Oncology, National Cancer Center Hospital, Tokyo, Japan, [2]Hamon Center for Therapeutic Oncology Research, The University of Texas Southwestern Medical Center at Dallas, Texas, USA, [3]Department of Genome Biology, Kinki University School of Medicine, Ohno-Higashi Osaka-Sayama, Osaka, Japan and [4]Division of Internal Medicine, National Cancer Center Hospital East, Kashiwanoha, Kashiwa, Chiba, Japan

Received October 26, 2006; accepted December 17, 2006

In order to review gene alterations associated with drug responses *in vitro* to identify candidate genes for predictive chemosensitivity testing, we selected from literature genes fulfilling at least one of the following criteria for the definition of '*in vitro* chemosensitivity associated gene': (i) alterations of the gene can be identified in human solid tumor cell lines exhibiting drug-induced resistance; (ii) transfection of the gene induces drug resistance; (iii) down-regulation of the gene increases the drug sensitivity. We then performed Medline searches for papers on the association between gene alterations of the selected genes and chemosensitivity of cancer cell lines, using the name of the gene as a keyword. A total of 80 genes were identified, which were categorized according to the protein encoded by them as follows: transporters ($n = 15$), drug targets ($n = 8$), target-associated proteins ($n = 7$), intracellular detoxifiers ($n = 7$), DNA repair proteins ($n = 10$), DNA damage recognition proteins ($n = 2$), cell cycle regulators ($n = 6$), mitogenic and survival signal regulators ($n = 7$), transcription factors ($n = 4$), cell adhesion-mediated drug resistance protein ($n = 1$), and apoptosis regulators ($n = 13$). The association between the gene alterations and chemosensitivity of cancer cell lines was evaluated in 50 studies for 35 genes. The genes for which the association above was shown in two or more studies were those encoding the major vault protein, thymidylate synthetase, glutathione S-transferase pi, metallothionein, tumor suppressor p53, and bcl-2. We conclude that a total of 80 *in vitro* chemosensitivity associated genes identified in the literature are potential candidates for clinical predictive chemosensitivity testing.

Key words: chemotherapy – sensitivity – drug resistance – solid tumor

INTRODUCTION

Malignant neoplastic diseases remain one of the leading causes of death around the world despite extensive basic research and clinical trials. Advanced solid tumors, which account for most malignant tumors, still remain essentially incurable. For example, 80% of patients with non-small cell lung cancer have distant metastases either at the time of the initial diagnosis itself or at the time of recurrence after surgery for the primary tumor. Systemic chemotherapy against malignant tumors remains of limited efficacy in spite of the development in the recent past of several new chemotherapeutic agents; therefore, patients with distant metastases rarely live for long (1).

Tumor response to chemotherapy varies from patient to patient, and clinical objective response rates to standard chemotherapeutic regimens have been reported to be in the range of 20–40% for most common solid tumors. Thus, it would be of great benefit it became possible to predict chemosensitivity of various tumors even prior to therapy. DNA, RNA and protein-based chemosensitivity tests have

For reprints and all correspondence: Ikuo Sekine, Division of Internal Medicine and Thoracic Oncology, National Cancer Center Hospital, Tsukiji 5-1-1, Chuo-ku, Tokyo 104-0045, Japan. E-mail: isekine@ncc.go.jp

been performed in an attempt to predict the clinical drug response, but the precise gene alterations that might be predictive of the chemosensitivity of the tumors are still unknown. Here we aimed to review the gene alterations that may be associated with the drug response *in vitro* (*in vitro* chemosensitivity associated genes) in order to identify candidate genes for predictive chemosensitivity testing in the clinical setting. The association between these gene alterations and clinical chemosensitivity in lung cancer patients has been reported elsewhere (2).

METHODS

In vitro chemosensitivity associated genes were identified from the medical literature as described previously (2). Briefly, we conducted a Medline search for papers on tumor drug resistance published between 2001 and 2003. This search yielded 112 papers, including several review articles. Manual search of these papers led to identification of 134 genes or gene families that were potentially involved in drug resistance based on their function. We conducted a second Medline search for *in vitro* studies of the 134 genes or gene families using the name of the gene as a keyword. Genes that fulfilled at least one of the following criteria for the definition of *in vitro* chemosensitivity associated gene were selected from the 134 genes: (i) alterations of the gene can be identified in a human solid tumor cell lines exhibiting drug-induced resistance; (ii) transfection of the gene induces drug resistance; (iii) down-regulation of the gene or of the protein encoded by it increases the drug sensitivity. For this last category, we included studies in which the gene expression or function was suppressed by antisense RNA, hammerhead ribozyme, or antibody against the gene product. Finally, a Medline search for papers on the association between gene alterations and chemosensitivity of solid tumor cell lines was performed using the name of the gene as a keyword. Papers in which the association was evaluated in 20 or more cell lines were included in this study. The name of each gene was standardized according to the Human Gene Nomenclature Database of National Center for Biotechnology Information (NCBI).

RESULTS

Of the 134 genes or gene families, gene alterations were found in cells exhibiting drug-induced resistance, transfection of the gene increased or decreased the drug resistance,

Table 1. Transporters and *in vitro* evidence of association with chemosensitivity

Gene symbol	Alterations in DIRC	Sensitivity of		Drugs	Association with chemosensitivity (cancer, drug)	Reference no.
		UCs	DCs			
ABCA2	U	–	S	Estramustine	–	1
ABCB1	U	R	S	DOX, PTX, VCR, VBL	Yes (lung, DOX)	2–11
					No (lung, DOX)	12
ABCB11	–	R	–	PTX	–	13
ABCC1	U	R	S	CPT, DOX, ETP, MTX, VCR	Yes (lung, CDDP, DOX)	11,14–21
					No (lung, PTX)	22
ABCC2	U	R	S	CDDP, DOX, MTX, VCR	No (lung, DOX)	18, 21, 23–25
ABCC3	NC, U	R	–	ETP, MTX	Yes (lung, DOX)	21, 25–28
ABCC4	NC, U	NC, R	–	MTX	No (lung, DOX)	12, 25, 29–31
ABCC5	NC, U	NC	–	DOX, MIT	Yes (lung, ETP)	12, 25, 31–34
ABCG2	M, U	R	–	DOX, MIT, MTX, SN38, TOP	–	35–43
MVP	U	–	NC	DOX	Yes (brain, CDDP, DOX)	44–47
					Yes (lung, DOX)	10
ATP7A	U	–	–	CDDP	–	48
ATP7B	U	R	–	CDDP	–	48–52
SLC29A1	U	–	–	5-FU	No (NCI-panel)	52, 53
SLC28A1	–	S	–	5′-DFUR	No (NCI-panel)	53, 54
SLC19A1	D	S	–	MTX	Yes (NCI-panel)	55–58

Alterations in drug-induced resistance cells (DIRC): D, down-regulated; M, mutated; NC, no change; U, up-regulated. Sensitivity of up-regulating cells (UCs) and down-regulating cells (DCs): NC, no change; R, resistant; S, sensitive.
Drugs: CDDP, cisplatin; CPT, irinotecan; DOX, doxorubicin; ETP, etoposide; MIT, mitoxantrone; MTX, methotrexate; PTX, paclitaxel; SN38, irinotecan metabolite; TOP, topotecan; VBL, vinblastine; 5-FU, 5-fluorouracil; 5′-DFUR, 5′-deoxy-5-fluorouridine, capecitabine metabolite.

Table 2. Drug targets, the associated proteins, and *in vitro* evidence of association with chemosensitivity

Gene symbol	Alterations in DIRC	Sensitivity of		Drugs	Association with chemosensitivity (cancer, drug)	Reference no.
		UCs	DCs			
*TUB*B	IEC, M	–	–	PTX	–	59–63
*TUB*B4	U	–	S	PTX	Yes (NCI-panel, PTX)	59, 60, 63–66
*TUB*A	IEC, M	R	–	PTX	–	64, 67, 68
*TYM*S	U	R	S	5-FU	Yes (renal cell, 5-FU)	69–74
					No (NCI-panel, 5-FU)	75
					Yes (lung, DOX)	10
*TOP*1	M	R*	–	CPT	–	76–84
*TOP*2A	M, D	–	–	ETP, DOX	No (lung, DOX)	10, 82–91
*TOP*2B	D	–	–	ETP	–	86, 87
*DHF*R	M, U	R*	–	MTX	–	92–96
*MAP*4	–	S	–	PTX	–	97
*MAP*7	–	S	–	PTX	–	98
*STM*N1	U	R	–	PTX	–	99, 100
*KIF*5B	–	R	R	ETP, PTX	–	101, 102
*HSP*A5	–	R	–	ETP	–	103
*PSM*D14	–	R	–	CDDP, DOX, VBL	–	104
*FPG*S	D	–	–	5-FU	–	105

Alterations in drug-induced resistance cells (DIRC): D, down-regulated; IEC, isoform expression change; M, mutated; U, up-regulated. Sensitivity of up-regulating cells (UCs) and down-regulating cells (DCs): R, resistant; S, sensitive. Drugs: CDDP, cisplatin; CPT, irinotecan; DOX, doxorubicin; ETP, etoposide; MTX, methotrexate; PTX, paclitaxel; VBL, vinblastine; 5-FU, 5-fluorouracil.
*Over-expression of the mutant gene.

and down-regulation of the gene altered the drug sensitivity for 45, 57 and 32 genes, respectively, and a total of 80 genes fulfilled the criteria for the definition of an '*in vitro* chemosensitivity associated gene'. The genes were categorized according to the protein encoded by them as follows: transporters ($n = 15$, Table 1), drug targets ($n = 8$, Table 2), target-associated proteins ($n = 7$, Table 2), intracellular detoxifiers ($n = 7$, Table 3), DNA repair proteins ($n = 10$,

Table 3. Intracellular detoxifiers and *in vitro* evidence of association with chemosensitivity

Gene symbol	Alterations in DIRC	Sensitivity of		Drugs	Association with chemosensitivity (cancer, drug)	Reference no.
		UCs	DCs			
*GSTP*1	U	–	S	CDDP, DOX, ETP	Yes (lung, DOX)	10, 106, 107
					Yes (NCI-panel)	108
GPX	–	R, NC	–	DOX	Yes (lung, CDDP)	109–112
GCLC	U	R	S	CDDP, DOX, ETP	Yes (NCI-panel)	106, 108, 113–121
*GGT*2	U	R	–	CDDP, OXP	–	114, 117, 122, 123
MT	U, NC	R	–	CDDP	Yes (urinary tract, CDDP)	118, 124–130
					Yes (lung, DOX)	10, 131
*RRM*2	U	R	–	5-FU, GEM, HU	–	71, 132–134
*AKR*1B1	U	–	–	DNR	–	135

Alterations in drug-induced resistance cells (DIRC): NC, no change; U, up-regulated. Sensitivity of up-regulating cells (UCs) and down-regulating cells (DCs): NC, no change; R, resistant; S, sensitive. Drugs: CDDP, cisplatin; DNR, daunorubicin; DOX, doxorubicin; ETP, etoposide; GEM, gemcitabine; HU, hydroxyurea; OXP, oxaliplatin; 5-FU, 5-fluorouracil.